Chapter 1

Confocal Laser Scanning Microscopy

1.1. Introduction

1.1.1. *Context and framework of chapter*

Confocal microscopy is a method of optical microscopy whose basic principle was described by Marvin Minsky in 1957 [MIN 57]. However, the practical implementation has not been easy and we had to wait until 1987 to see the appearance of the first commercial system of confocal laser scanning microscopy [WHI 87]. Today, a complete system of confocal laser scanning microscopy is a complex system that uses cutting-edge optical components, electronics, electromechanical and computer technology. For over 25 years, owing to its flexibility and performance, this method of optical microscopy has generated keen interest in the community of researchers in biology. Industrial researchers in optics, chemistry, nanoscience, electronics, computing and image processing have also promoted the evolution of this tool by offering technological improvements or developing new types of fluorescent probe, unusual modes of use, but also through derived techniques, simply based upon a more controlled and quantitative use, or on the implementation of complex photonic approaches that give resolutions of the order of tens of nanometers, well below the impassable diffraction limit!

Chapter written by Thomas OLIVIER and Baptiste MOINE.

Faced with the complexity, the various methods of implementation and the numerous methods derived from confocal laser scanning microscopy, it would be very presumptuous to claim to be exhaustive in these few pages. An example of the restrictions we have chosen to adopt is noticeable from the title of this chapter: "Confocal Laser Scanning Microscopy". The title immediately eliminates other approaches capable of achieving *optical sectioning microscopy*[1] such as spinning disk microscopy (or Nipkow disk) or others not using scanning, but a particular pattern of illumination. These methods do not achieve the flexibility, sensitivity and resolution of the confocal laser scanning microscope but still remain very interesting for their speed and reduced cost. This restriction being made, there are still many things to say. However, the purpose of this chapter is not to describe one-by-one the many applications and methods derived from confocal microscopy, nor to present the alternative technologies developed by different manufacturers. Let us simply note that there are many ways to use confocal microscopy and there are many technological solutions to develop a confocal microscope. Despite all of this, there are still some common denominators for most of the systems and most of the applications.

In the first part of this chapter, we will therefore attempt to lay the foundation for understanding the general principle of this optical method. We will endeavor to highlight some key elements of the current systems of confocal microscopy with emphasis on their role and operating principle. Then we will take a few illustrative examples to describe and discuss the advantages and limitations inherent in this method when used with biological media. This part will require a brief introduction recalling some notions of biology and fluorescent labeling. Finally, we briefly describe the main derived or related techniques. We will focus in particular on nonlinear contrast microscopy and we conclude this chapter by referring to the latest advances that have enabled us to achieve optical resolutions below the diffraction limit.

1 As we will see later, confocal microscopy allows capturing images using only the light coming from a slice of the order of 1 micron thickness in a sample. This allows obtaining what is called in biology "serial sections" without physically cutting the sample into thin slices, as is usually the case in histology.

1.1.2. *From wide-field microscopy to confocal microscopy*

Before entering the heart of the subject and talking about confocal microscopy, it is necessary to recall some generalities regarding wide-field optical microscopy. The objective of this section is to place confocal microscopy within the overall context of optical microscopy for biology. This section requires some prerequisites on wide-field microscopy. For more information on the subject, the reader is referred to more detailed books [WAS 94].

Historically, we assign the creation of the first true optical microscope to the Englishman Robert Hooke, who in 1665 published a book [HOO 65] presenting his first observations, in particular of insects and plant cells. Shortly afterwards, it was the Dutchman Antoni Van Leeuwenhoek who, being passionate about the discoveries of Hooke, built his own microscopes capable of achieving a magnification greater than 200, whilst Hooke's microscope only reached a magnification of the order of 30 to 50. Under these conditions, Leeuwenhoek observed for the first time micro-organisms such as protozoa, spermatozoid or even blood cells. Thus, from its introduction, the optical microscope immediately became the prime tool for biologists in bringing about major discoveries about the basic organization of life.

Today, we can obtain magnifications of more than one thousand with a classical optical microscope and this is only finally five times more than Leeuwenhoek's magnification, whilst technological progress has been considerable over 300 years! Indeed, technological and theoretical evolutions of optics have allowed us to achieve objectives of better quality, composed of well thought-out assemblies of lenses to reduce the number of aberrations. These aberrations are very annoying, especially in microscopy since we seek to have both a very high magnification and a high numerical aperture, which requires working very far from the paraxial approximation. Today, microscope objectives are virtually free of any optical aberration and resolution is only limited by the phenomenon of diffraction. The ability to collect a large amount of light has also been pushed little by little to its maximum and today we find immersion objectives with a numerical aperture typically equal to 1.4, which corresponds to a total angle of collection near 180° (one can hardly expect better with only one objective!). The optical resolution then follows directly from the diffraction limit which itself depends upon the numerical aperture. In the best possible observation

conditions, the theoretical resolution of optical microscopes can hardly fall below 150 nm (except in exceptional cases that we will discuss later...). This limit of resolution imposed by diffraction explains why it is not necessary to have magnifications higher than 1,000 because they would just increase the diffraction pattern without providing additional information on the sub-structure of the observed object (even if today it is sometimes possible to deconvolve the images digitally to gain a little more resolution).

In the 20th Century, improvements were rather more focused on contrast. Indeed, to evaluate the performance of an imaging device, the notion of contrast is inseparable from the notion of resolution. Having a theoretical resolution of about 150 nm is one thing, but how can we distinguish a small transparent object immersed in another transparent medium with a very close refractive index? Apart from a few exceptions, like red blood cells, the cells are often transparent and largely made up of water. To work around this problem, we have to use optical contrast agents, that is to say, colored probes, which have affinities for different tissular, cellular or intracellular structures. However, when the biological environment must remain alive, this type of labeling is often prohibited in order to not alter cellular functions.

For this purpose, other techniques have gradually emerged such as dark field microscopy, phase contrast microscopy (recipient of the Nobel Prize for Physics in 1953 for Frederik Zernike) and differential interference contrast microscopy. Without going into too much detail, let us recall that dark field microscopy is based upon elimination of the straight light to collect only the light scattered by the samples whilst phase contrast microscopy or interferential contrast microscopy use an interference phenomenon to transform a heterogeneity of the refractive index into a gray level variation. Finally, fluorescence microscopy, or more particularly epi-fluorescence microscopy, has brought a new type of interesting approach. In this technique, the sample is tagged with dyes which also have fluorescent properties (see the section on fluorescence below). The optical principle consists of illuminating the sample with a light corresponding to the absorption bands of the fluorophore, then filtering the excitation light and collecting only the light emitted by fluorescence at greater wavelengths. Hence, any labeled area appears bright on a black background. This approach seems to provide an alternative type of contrast to wide-field contrasts with colored tagging and yet there is a fundamental difference between these two modes of observation. Indeed, in bright-field microscopy,

it is about observing colored elements on a white background. This is not necessarily easy when tagged objects are very small, since the power of light transmitted decreases exponentially with the thickness crossed (Beer-Lambert law). It is a matter of identifying a small lightly-colored dot on a white background. In contrast, in fluorescence, it is necessary to identify an object, although weakly luminous, but on a black background. This method of observation is potentially much more sensitive. If the filtering of the excitation light was done well and the object is sufficiently fluorescent, nothing, in fact, prevents localizing an object of a size much smaller than the resolution. Thus, with the use of very sensitive cameras allowing photon counting, it is now possible to localize a single molecule with this kind of method [MOE 03].

In this context, confocal microscopy was born as an answer to another problem, which has so far not been addressed: the depth of field of microscopes. For a given focus, the depth of field corresponds to the longitudinal extent (in the direction of the optical axis) within which an object can still be imaged clearly by the imaging system. As any good amateur photographer knows, the depth of field is much weaker when the subject is close and the aperture of the system is high. However, microscopy pushes this case to the extreme! The depth of field is then typically of the order of a micron, or even a few hundred nanometers for immersion objectives of high numerical aperture. Consequently, when working at high magnification and high numerical aperture, it is almost impossible to have all the planes of the sample sharp at the same time. This is one of the reasons why biologists work with thin slices of biological tissue. These tissue slices must be prepared with great care before being placed between slide and coverslip. The equipment for making these fine cuts (vibratomes, cryomicrotomes, etc.) barely allows thicknesses of less than 5 or 10 microns, which in fact correspond to the thickness of a cellular layer. Hence, even in the case of a single cellular layer, the effect of a weak depth of field for microscopes can be observed and all the intracellular structures cannot be sharp at the same time. The principle of confocal microscopy is precisely to take advantage of the weak depth of field of microscopes to make virtual slices of submicron thicknesses. For this, the basic principle is to use a simple hole for spatial filtering to eliminate the light coming from planes outside the limits of the depth of field. The directly significant and most obvious benefit of this method is to provide an axial resolution (along the optical axis of the microscope) which is more controlled. We will see later that this property allows us to improve the contrast and to take full advantage

of the theoretical resolution of optical microscopy. In addition, coupled with the production of a series of images, the axial resolution allows also us to virtually extend the depth of field or to perform three-dimensional reconstructions of biological objects. These advantages of the confocal microscopy configuration have brought to optical microscopy a more controlled and quantitative dimension. Consequently, confocal scanning laser microscopy was able to evolve and has been the starting point for many technological and methodological developments exploiting complex mechanisms of light-matter interactions for research in biology and medicine. However, and this is the whole purpose of this chapter, we will see that if the basic principle seems simple enough, confocal scanning laser microscopy is a fairly complex method to implement and suffers from several artifacts and limitations. It is therefore essential to understand not only its mode of operation, but also its limitations to make the most of its capabilities and use it to answer scientific questions that could not be explored otherwise.

1.2. Principle and implementation

We have seen that the essence of confocal microscopy is to reduce the number of planes observed along the optical axis in order to take into account only those whose sharpness is sufficient, in other words, those which are in the depth of field. In fact, in fluorescence contrast, the laser beam will generate a signal from the sample all along its path. However, if we calculate the typical depth of field of a high numerical aperture microscope (NA = 1.4) for 550 nm radiation, it gives a value of about 430 nm (how to obtain such a value will be discussed later on). It seems obvious that, in a sample exceeding ten microns (size of a typical animal cell), most of the light collected by the microscope does not come from planes localized in the depth of field and so blurs the image.

If we take a sample that is thicker and more scattering, the picture darkens. Indeed, much of the light coming from the object plane will now be scattered, refracted or reflected on the path back towards the objective. It therefore seems to be coming from the last scattering point and not the place where it was actually emitted. Consequently, in the final observed image, the light contribution from planes that are outside the object plane will be predominant and it will then become increasingly difficult to achieve a sharp and contrasted image. Optical researchers have had to develop methods to

overcome this spurious signal and to image at greater depths in samples which are more scattering (which proved to be a necessity in the study of biological tissues). These developments have given rise to several microscopy systems allowing real virtual slices of the sample to be made, gathered under the name of Optical Sectioning Microscopy (OSM). Among these different techniques, we shall denote fluorescence microscopy by multiphotonic excitation [DEN 90] as well as different computational optical sectioning microscopy (COSM) [CON 05].

In this chapter, we will focus on the study of one of these techniques, confocal scanning laser microscopy, which is certainly the most commonly used.

1.2.1. *General principle*

To build a confocal laser scanning microscopy setup, a number of modifications were made to the classical setup, but part of the principle remains the same. A sample is illuminated, and an objective lens collects the light, either reflected or emitted (in the case of fluorescence) by the sample. Although one can imagine that numerous setups exist allowing the implementation of this kind of technique, everything can be reduced to a similar basic schema (Figure 1.1).

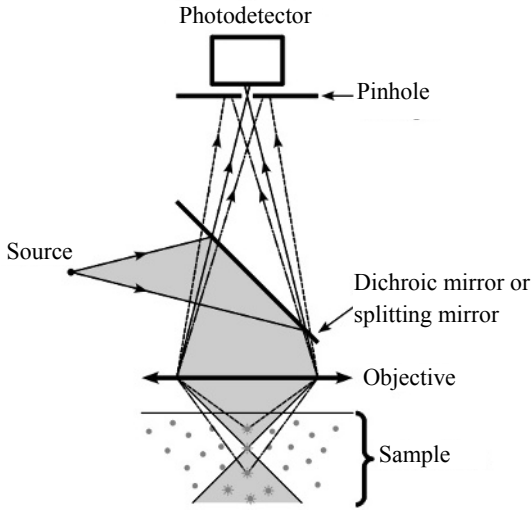

Figure 1.1. *General principle of confocal microscopy*

A light source, most of the time a laser, is brought through a dichroic mirror or a semi-reflecting mirror to the objective. The beam is then focused on the sample and illuminates it with a spot whose size depends upon the different phenomena of diffraction undergone when crossing the optics of the microscope. The most common approximation is to assume that the objective is primarily responsible for the formation of this spot. Accordingly, knowing some of its characteristics (numerical aperture (NA) or aperture number, index of immersion of the medium), we can deduce the size of the diffraction spot and therefore the illuminated area of the sample. It can vary between 2 microns for an infrared beam with a 0.25 numerical aperture air objective, to 170 nm for a near UV beam with a 1.4 numerical aperture oil immersion objective.

The reflected light or fluorescence emitted by the sample (depending upon the type of contrast that we wish to observe) is then collected by the objective. The light signal is separated from the excitation by a dichroic mirror, and is then focused on a pinhole located just in front of the detector. This aperture is in the image plane conjugate to the object plane of the lens, and is called a confocal pinhole. Its size can vary between 10 and 500 microns depending upon the type of objective used and the required resolution. Thus, the light coming from a point source which is not in the conjugate plane with the confocal pinhole is partially removed through this pinhole. The collected light then originates essentially from the conjugate plane with the confocal pinhole.

With this device, we record the light signal coming from a point in our sample, in other words, one single “pixel” of the image. To obtain a true two-dimensional image, it is necessary to add a system which allows scanning point-by-point. Then two solutions appear: either the sample is moved by means of a raster scanning stage or the laser beam is deflected and scans the sample through different optical devices (galvanometer mirror scanner, spinning disk). Both techniques have their advantages and disadvantages. The scanning of the sample allows the production of quite homogeneous images, but is limited by the speed and accuracy of the motion of the stages. In addition, such motion can be difficult in the case of bulky samples. Laser scanning, meanwhile, is not concerned with the size or nature of the sample and can be performed at a much higher speed and accuracy. However, since the laser beam can be moved away from the optical axis, off-axis aberrations and vignetting may occur, making the image inhomogeneous.

The recording of an image point-by-point first of all has the advantage of limiting the scattering of unwanted light which can come from areas adjacent to the point imaged because they are simply not excited. Thus, for example, we found experimentally that a scanning laser microscopy image (even without the confocal filtering) appears more contrasted and less noisy than an epifluorescence wide-field image. The addition of the confocal pinhole to filter the photons coming from areas outside the depth of field allows us to further increase the sharpness, and especially, the contrast of the image. The latter corresponds to a transversal optical cross-section of the sample. We will see, in the next section, that the use of a confocal pinhole whose size is perfectly suited to the diffraction pattern given by a point source can also greatly improve the theoretical resolution of the device. There are still some limitations in principle with this type of confocal microscopy. Indeed, the mere fact that the focal volume is extremely small (sometimes only a few femtoliters!) implies that the number of photons emitted or scattered by this small volume is often very low. The excitation and detection of such a weak signal then requires the use of intense sources (lasers), highly sensitive detectors, and the use of high speed image acquisition. All this imposes certain limitations and complicates the implementation of this method and leads to a high cost.

By now moving the sample or the objective lens axially (along the optical axis), we can then produce a series of optical slices, that is to say, recording the images from different virtual sections of the sample. The probed volume can, using software, be rebuilt in three dimensions. Thanks to this type of microscopy, it is no longer necessary to work on thin samples or slices of samples. However, even on thin sections of samples (typically greater than 5 microns), the axial resolution of confocal microscopy will remain very low and it proves interesting to reconstruct images having a minimal and identical resolution throughout the thickness of the imaged sample.

1.2.2. *Axial and lateral resolution in confocal microscopy*

Any optical device has a certain optical resolution. It can be defined in many ways, but it is usual to say that it corresponds to the size of the smallest measurable object. It can also correspond to the distance between the two closest dots separable by the optical system. These two definitions are very similar. The second allows us to glimpse a way to calculate or estimate this resolution. This requires knowledge of the shape of the image

of a point through our optical system. In general, a point never gives another point for an image, but a spot whose amplitude distribution is described by a function called Point Spread Function (PSF). This is equivalent to the impulsional response in an electrical circuit. If we know the PSF, it is possible to deduce the minimum distance between two point sources on the object plane necessary to maintain two PSFs distinguishable in the image plane. The other benefit of this PSF is that the image of a sample on the detector is simply the convolution of its transmission function with this same PSF. It allows us to calculate *a priori* the type of image expected. This function is the response of the instrument to a light spot and it depends upon the three coordinates x, y and z describing the object space. Also, regardless of the instrument, it is possible to describe both a lateral resolution in the plane (O, x, y) and an axial resolution along the axis (Oz) (optical axis). However, bear in mind that we want to calculate this kind of response for microscopy and in particular for confocal microscopy. In this type of technique, the PSF will be a function with cylindrical symmetry, as is the instrument that generates it.

1.2.2.1. *Lateral resolution*

Although this chapter deals with confocal microscopy, it is necessary to lay the bases for this problem in conventional microscopy, and then extend it to confocal microscopy. A sample is illuminated, and then the light emitted or reflected by this is collected by the objective lens before hitting a detector. When a microscope is properly designed, it is commonly accepted that the resolution is limited by the diffraction of light by the pupils of the different optical elements. Most often, it is the pupil of the objective lens which is the limiting factor of the system. The image of a point is no longer effectively a point but a diffraction spot in the image plane, due to a pupil, the characteristics of which will depend upon the wavelength. Using the diffraction theory of Rayleigh-Sommerfeld and remaining within the paraxial approximation, it can be shown that the amplitude of the electrical field in the image plane corresponds to the Fourier transform of the transfer function of the pupil [BOR 99]. It has the shape of an Airy function:

$$\mathrm{PSF}_{\mathrm{class}}(\nu) = \frac{2\mathrm{J}_1(\nu)}{\nu} \qquad [1.1]$$

where $\mathrm{J}_1(\nu)$ represents the first Bessel function, ν the normalized distance to the optical axis $\left(\nu = k \cdot r \cdot n \cdot \sin(\theta_0)\right)$, k is the wave number $(k = 2\pi/\lambda)$,

λ is the wavelength, r is the distance to the optical axis, n is the refractive index of the medium between the objective lens and the object plane and θ_0 the angle between the optical axis and the steepest beam from the point source able to enter the objective lens and emerge. This function has a maximum when $\nu = 0$, and its first cancellation falls when $\nu = 3.832$, by:

$$r = \frac{0.61 \cdot \lambda}{n \sin(\theta_0)} = \frac{0.61 \cdot \lambda}{NA} \quad [1.2]$$

where NA is the numerical aperture of the objective $\left(NA = n \sin(\theta_0)\right)$.

In this approximation, the image made by a microscope of a point source of light therefore corresponds to the function described above. From this result, we can go back to the resolution: the minimum distance between two points such that their images are just distinguishable from each other. It is necessary to take into account what is seen by the detector, namely, the intensity of light which is in fact the squared modulus of the PSF:

$$I(\nu) = \left[\frac{2J_1(\nu)}{\nu}\right]^2 \quad [1.3]$$

To establish when two images are separated, there are two criteria: that by Rayleigh and the one by Sparrow. The first, which is the most widely used, states that two point sources can be separated if the center of the first image is outside the central spot of the diffraction of the second. This is, of course, valid for incoherent point sources. If they are coherent, their dephasing can improve (out of phase) or decrease (in phase) the resolution by interference. In addition, there are cases where the criterion, expressed in this way, can no longer apply. If, for example, the functions to be separated have a Gaussian profile, the criterion collapses since the concept of cancellation of the profile makes sense only to infinity. Thus, you can redefine the Rayleigh criterion as follows: two points of equal brightness are separated if the intensity drops by at least 26.5% between their two images [HEC 02]. This corresponds to the intensity drop observed when two Airy functions are just separated. Following this criterion, we find a resolution of the order of:

$$d_{\text{lateral}}(\text{Rayleigh}) = \frac{0.61 \cdot \lambda}{NA} \quad [1.4]$$

For the Sparrow criterion, we consider two point sources A and B emitting an equal light intensity and forming two images A' and B' in the plane of the detector. They are separable if the intensity received by the detector in the middle of the segment A'B' is equal to the intensity received at A' in the absence of point B (and vice versa) [HEC 02]. The advantage of this criterion is that it can be generalized to coherent sources whilst the Rayleigh criterion is implicitly based upon the incoherence of sources. Logically, it would be necessary to calculate the Sparrow criterion, to consider the images obtained by reflection contrast as coherent images since they come from the reflection of a source that is itself coherent, whilst the fluorescence images must be considered as incoherent. For simplicity, we assume here that whatever the mode, the imaging is incoherent, and finally, the Sparrow criterion is similar to a 3 dB attenuation. In this case, the resolution is none other than the full width at half-height of the PSF being:

$$d_{\text{lateral}}(\text{Sparrow}) = \frac{0.51 \cdot \lambda}{\text{NA}} \qquad [1.5]$$

Turning now to the case of the confocal microscope, we have seen its principle roughly, which consists of illuminating a sample and collecting light emitted or reflected via the same objective. The fluorescence signal or reflection is then focused and filtered through a pinhole and collected by a detector. Since the resolution depends directly upon the wavelength, we will have to distinguish reflection contrast microscopy from fluorescence contrast microscopy. In reflection, the excitation and collected radiation is the same. We will call both of them λ_{exc}. In fluorescence, the sample is excited at a first wavelength, λ_{exc}, which causes the emission of a new radiation whose wavelength is greater, λ_{em}.

In any case, we can split the problem by considering on the one hand excitation and on the other hand detection. In confocal microscopy, the illumination of the sample is done by a parallel beam, which we shall assume is Gaussian (Figure 1.2). It passes through the objective lens and is then focused at point P0 of the object plane in a spot owing to the diffraction by the entrance pupil of the objective. The illumination is therefore done point-by-point as we have seen above. By using the Rayleigh-Sommerfeld diffraction theory, the field reflected by the sample can be described as follows [BOR 99]:

$$E(x,y) = PSF_{ill}(x,y) \cdot r(x,y) \qquad [1.6]$$

where r (x, y) is none other than the function characterizing the reflection of the sample. The expression of this field involves the illumination PSF corresponding to a portion of the total PSF.

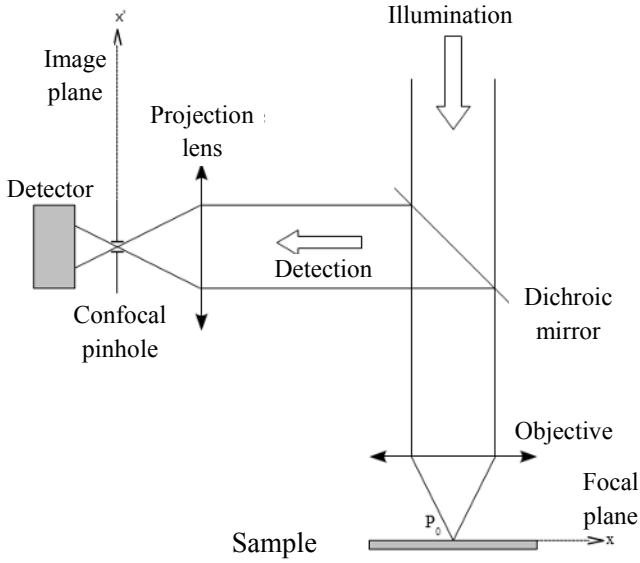

Figure 1.2. *Schematic of the system used for the calculation of the PSF (illumination with a collimated beam)*

The field in the image plane is, meanwhile, the convolution of the reflected field at the sample with the PSF corresponding to the optical detection made with the same objective and a focal lens in front of the confocal pinhole:

$$E'(x',y') = \left(\left[PSF_{ill} \cdot r\right] * PSF_{det}\right)(x',y') \qquad [1.7]$$

If we consider, once again, that the objective is the main limiting factor, we can imagine that this second PSF is identical to the first and, finally, identical to the PSF obtained in classical microscopy (PSF_{class}). Hence, the field in the image plane is only going to depend upon the characteristics of the objective and the size of the confocal pinhole.

To use the microscope in optimal conditions, it is necessary that the diameter of the confocal pinhole is less than a quarter of the diameter of the Airy disk created by the objective. Under these conditions, a final

simplification occurs and we find, finally, in the image plane, an intensity of this shape [COR 96]:

$$I_{conf} = \left(\left(PSF_{class} \right)^2 * r \right)^2 \quad [1.8]$$

Finally, by reducing our sample to the study of a reflecting point (a Dirac point), we can establish that the PSF of the total system (PSF_{conf}) is the PSF found in the case of the classical microscope, squared. It is therefore expressed through the Bessel functions:

$$PSF_{conf}(\nu) = \left[\frac{2J_1(\nu)}{\nu} \right]^2 \quad [1.9]$$

The intensity of a reflected point in the image plane is thus:

$$I(\nu) = \left[\frac{2J_1(\nu)}{\nu} \right]^4 \quad [1.10]$$

It is very common to see the full width at half maximum of this function as a basis for calculating the resolution in confocal microscopy. This is expressed below and appears to be thinner than in a conventional system. However, this result does not necessarily mean that the resolution (separation of two points) is inherently better in confocal microscopy, especially whilst calculating the latter when taking account of the Sparrow criterion:

$$d_{lateral}(3dB) = \frac{0.37 \cdot \lambda_{exc}}{NA} \quad [1.11]$$

This function has exactly the same minima of intensity calculated by classical microscopy, but it decreases more rapidly. Indeed, the second formulation of the Rayleigh criterion proves to be essential. We can therefore apply the two usual criteria that give us the following two resolutions [COR 96]:

$$d_{lateral}(Rayleigh) = \frac{0.56 \cdot \lambda_{exc}}{NA} \quad [1.12]$$

$$d_{lateral}(\text{Sparrow}) = \frac{0.51 \cdot \lambda_{exc}}{NA} \quad [1.13]$$

These two theoretical values for resolution are valid in reflection contrast microscopy. We note that according to the Rayleigh criterion, the resolution is slightly better because of the greater sharpness of the PSF. However, according to the Sparrow criterion, we find the same resolution as in classical microscopy.

Regarding the fluorescence images, it is necessary to differentiate the illumination PSF, calculated using the wavelength of excitation, from the detection PSF calculated using the emission wavelength. The easiest way is to use the above formulas by taking an average wavelength expressed as follows:

$$\tilde{\lambda} = \sqrt{2}\frac{\lambda_{exc} \cdot \lambda_{em}}{\sqrt{\lambda_{exc}^2 + \lambda_{em}^2}} \quad [1.14]$$

It is necessary, however, to make an important remark. Let us imagine that, for the purpose of the experiment (light signal very weak for example), the confocal pinhole is relatively open. If its size is greater than the diameter of the Airy disk, then two points close to each other will be separated only if the illumination separates them. In this case, the PSF of the total system is identical to the illumination PSF and, therefore, to that obtained by classical microscopy. This applies even if the size of the pinhole is small but the illumination is not correctly focused and thus is uniform on the sample:

$$PSF_{conf}(v) = PSF_{class}(v) = \frac{2J_1(v)}{v} \quad [1.15]$$

We deduce that the resolution, within the meaning of the two criteria mentioned above, is:

$$d_{lateral}(\text{Rayleigh}) = \frac{0.61 \cdot \lambda_{exc}}{NA} \quad [1.16]$$

$$d_{lateral}(\text{Sparrow}) = \frac{0.51 \cdot \lambda_{exc}}{NA} \quad [1.17]$$

For the images in reflection contrast, the resolution of the confocal system is the same as that of a conventional system. In fluorescence contrast

and in classical microscopy, the excitation covers the entire field and the resolution comes from the fact that the detection of fluorescence by the objective is done on a receptor discretizing spatially where the different photons arrive. This depends upon the wavelength of emission of the sample. In confocal microscopy, the detector receives all the photons passing through the pinhole and makes no distinction as to their origin. It is this excitation which enables us to obtain a lateral resolution. This depends upon the excitation wavelength and is slightly improved over the conventional case by a factor $\lambda_{exc}/\lambda_{em}$.

1.2.2.2. *Axial resolution*

With the lateral resolution, we can define the axial resolution as follows: it is the length of the smallest measurable object along the optical axis. In other words, it is the shortest distance between two points distinguishable along the optical axis. It is important to keep in mind these criteria, the overall PSF of the instrument is no longer necessarily the function that allows us to calculate the resolution of the device.

We have repeatedly stated that confocal microscopy allows us to make optical sections of a certain thickness. This arises because the confocal pinhole lets through only the radiation from the object plane, or very close planes. In the following, it will be shown that the thickness along the optical axis of this optical section can be likened to the resolution, although this is not always the case.

Consider, initially, an example of a classical microscope. We do not, in this case, achieve optical slicing since the light coming from all planes is collected on the camera. However, this microscope has some form of axial resolution since we can measure the distance between two objects along the optical axis, if they are far enough away not to be sharp with the same z setting. In this case, we say that the resolution is related to the depth of field (DOF). The latter is a parameter corresponding to the distance between the nearest sharp plane and the farthest one from the microscope. Indeed, the image of a point object outside the object plane is in fact a pattern. As this does not exceed a certain size (about 30 microns), it can be considered that the eye, or any other sensor, records a sharp image. We can therefore calculate, through optical geometry, the value of this depth of field as a function of the numerical aperture of the objective, the wavelength of the

radiation used, and the refractive index of the medium between the object plane and the objective:

$$PDC = \frac{n \cdot \lambda_{em}}{NA^2} \qquad [1.18]$$

In confocal microscopy, the influence of the size of the filtering pinhole is paramount, as for calculations of the axial resolution. It fixes directly the axial extent of the imaged area, in other words, the thickness of the optical sections obtained. We will distinguish here two cases: the first when the size of the pinhole is less than one quarter of the width of the Airy disk, and the second when it is greater than the width of the Airy disk.

In the first case, the approximation of the optical geometry is not enough and it becomes necessary to take into account diffraction effects. Consider a reflector plane, placed in the focal plane of the objective, and move it along the optical axis. It is quite easy, using scalar theory and paraxial approximation, to show that the intensity along the z-axis at the detector then evolves as follows [COR 96]:

$$I_{plan}(z) = \left[\frac{\sin\left(nkz\left(1-\cos\theta_0\right)\right)}{nkz\left(1-\cos\theta_0\right)} \right]^2 \qquad [1.19]$$

The depth of field is then described as the width at half maximum of this function and acts as the resolution. This type of model is perfectly suited to the study of an area or more generally an interface in confocal reflection contrast microscopy. Note that in this special case, the resolution and the axial size of the optical section are given by the same relationship:

$$d_{axial}(3dB)_{plan} = \frac{0.90 \cdot n \cdot \lambda}{NA^2} \qquad [1.20]$$

If we now consider a punctual reflector, for example particles suspended in a fluid, we obtain a different response in intensity along the z-axis. Indeed, it is necessary to take into account the propagation to the punctual reflector and the reflection of the light on it and the return path through the objective. The objective is again assumed to be uniformly illuminated and we always work within the case of paraxial optics. We can then use the calculation above. We find a new expression for the intensity giving a new

resolution that is generally used in confocal reflection microscopy [COR 96]:

$$I_{point}(z) = \left[\frac{\sin\left(\frac{nkz}{2}(1-\cos\theta_0) \right)}{\frac{nkz}{2}(1-\cos\theta_0)} \right]^4 \quad [1.21]$$

$$d_{axial}(3dB)_{point} = \frac{1.24 \cdot n \cdot \lambda}{NA^2} \quad [1.22]$$

Finally, it is interesting to note that the axial resolution for a punctual reflector is 1.38 times greater than for a plane reflector, all other things being equal. In addition, when we are away from the focal plane, we can see that the intensity drops to $1/z^4$ for a punctual reflector and $1/z^2$ for a plane reflector. Consequently, the contribution of small reflective particles away from the imaging plane is less likely to blur the image if it is a surface.

We have calculated two possible values for the resolution, one for a plane reflector, the other for a punctual reflector in the case where the confocal pinhole is really adapted to the Airy disk. However, in biology, most of the time, the microscope is used in fluorescence contrast, so we need to recalculate the resolution, in this case. Let us first attempt to understand the modifications generated by observation in fluorescence mode. Obviously, the incident wavelength on the sample will not be the same as the one collected by the objective and focused on the confocal pinhole. This implies a modification in the intensity along the optical axis at the detector such that [COR 96]:

$$I_{point}(z) = \left[\frac{\sin\left(\frac{nk_{exc}z}{2}(1-\cos\theta_0) \right)}{\frac{nk_{exc}z}{2}(1-\cos\theta_0)} \right]^2 \cdot \left[\frac{\sin\left(\frac{nk_{em}z}{2}(1-\cos\theta_0) \right)}{\frac{nk_{em}z}{2}(1-\cos\theta_0)} \right]^2 \quad [1.23]$$

where, $k_{exc} = (2\pi)/\lambda_{exc}$ and $k_{em} = (2\pi)/\lambda_{em}$. By taking $\lambda_{exc} = \lambda_{em}$, we find the same expression as that obtained for a punctual reflector. To simplify things, we take, in fluorescence contrast, an average wavelength between emission and excitation. This is consistent with what we saw for lateral resolutions:

$$d_{axial}(3dB)_{point} = \frac{1.24 \cdot n \cdot \tilde{\lambda}}{NA^2} \quad [1.24]$$

$$\tilde{\lambda} = \sqrt{2}\frac{\lambda_{exc} \cdot \lambda_{em}}{\sqrt{\lambda_{exc}^2 + \lambda_{em}^2}} \quad [1.25]$$

From the above equation, we see that $\tilde{\lambda}$ is greater than λ_{exc}. Also, the resolution of fluorescence contrast is slightly worse than in reflection.

We now turn to the case where the filtering pinhole is larger than the radius of the Airy disk. Placing a confocal pinhole allows us to obtain an optical section by rejecting the light coming from planes relatively far from the objective focal plane. However, the resolution of the device does not correspond to the width of this optical section. The thickness of the optical section (l) will correspond to the width at half height of the intensity distribution after the confocal hole. This width depends, on the one hand on, upon an optical wave parameter coming from diffraction of the fluorescence emission or reflection (depending upon the contrast used) and on the other hand a geometrical optics parameter owing to the effect of the pinhole (the second term under the square root):

$$\ell = \sqrt{\left(\frac{1.77 \cdot \lambda_{em}}{NA^2}\right)^2 + \left(\frac{\sqrt{2} \cdot n \cdot a}{NA}\right)^2} \quad [1.26]$$

where a is the diameter of the filtering pinhole.

The confocal pinhole is too large to affect the separation of two points relatively close to each other. The signals coming from these two points will go through the hole regardless. Consequently, the resolution only depends upon the laser excitation and is this time different from the thickness of the optical section. In fact, if you want to separate two points, it is necessary to excite them separately. The resolution corresponds to the width at half height of the illumination function along z (3 dB attenuation criteria). We find:

$$d_{axial}(3dB)_{pinhole > 1 \cdot Airy} = \frac{1.77 \cdot \lambda_{exc}}{NA^2} \quad [1.27]$$

1.2.2.3. *Discussion concerning the theoretical and experimental resolutions*

Whichever model is considered, the lateral resolution is inversely proportional to the numerical aperture of the objective used, and to the square of it, axially. We can therefore improve the resolution in both directions using an immersion objective, which is to say by not imaging in air, but in a liquid of relatively high index. The two most common are water and oil with respective refractive indices of 1.33 and 1.52.

Note that the formulas listed above, in general, remain theoretical formulas. Experimentally, the resolution will always tend to be poorer [KOZ 01, STE 98]. However, we can approach the theoretical values by spatially deconvolving the signal collected on the detector [YOO 06]. We will see in the next section, which is more applied, the limits of this theory and the experimental phenomena influencing this resolution. They are only valid of course when the microscope is used under the conditions specified by the manufacturer of the objective. In previous calculations, we relied on the principle that the image of a point source corresponds exactly to the diffraction pattern of the objective pupil (image limited by diffraction and without aberrations). In reality, it is very rare to use an objective in such conditions. The biggest aberrations that we will meet in biology are in fact owing to significant gaps in refractive index. This is inherent to the sample (inhomogeneities in the refractive index) or the result of a wrong choice for the coverslip or the immersion medium for a particular objective.

We can go further; since it has been shown, theoretically and experimentally, that if an objective is used with an unsuitable coverslip or immersion medium, or if the detector is not placed exactly in the image plane, then the resolution and image contrast will be affected. To find a resolution closer to reality in confocal microscopy, it is necessary to use a model involving these different modes of use. Several teams have developed such models using geometrical optics and/or optical physics to predict the image of a point source under different optical conditions [GIB 91, HAE 04, TOR 97].

Taking into account the expression of the Sparrow and Rayleigh criteria, it appears that the resolution and contrast are intimately linked. In other words, whatever affects one will affect the other. Detection plays an important role in the contrast of the image and therefore upon the resolution.

Pixelization and the elevated signal-to-noise ratio therefore have negative effects upon the resolution [STE 98].

In all the calculations that we have made, we have always sought to determine the resolution on the optical axis. In confocal microscopy, the point where the laser focuses is scanned in the plane that needs to be imaged. The microscope is not a totally invariant system and the PSF changes slightly when the source point moves in the object space. From a lateral (we talk about resolution) view, the astigmatism, coma and field curvature will cause a loss of resolution when the imaged point is far from the axis (edge of the images). When the optical elements are properly corrected, the loss will be small, until becoming negligible.

Regarding axial resolution, the objective having symmetry of revolution along the optical axis, there can only be two conjugate planes so that an object in one of these planes creates an image without aberration in the other. For an immersion objective used in biology, this plane is usually positioned by the manufacturer behind the microscope coverslip. Thus, when working with high numerical aperture, the aberration caused by a slightly different or the absence of a coverslip can be very important.

Finally, it is important to differentiate what we can see from what we can resolve. Indeed, a sub-resolution fluorescent object in a dark environment can be detected, that is to say, observed. Its presence is already information for us, we can also imagine measuring its intensity as a number of counts. We cannot however consider this object resolved, i.e. we cannot measure its size, nor say whether it is one or several objects.

1.2.3. *Some notions of fluorescence*

In confocal microscopy, we essentially use two types of contrast, imaging by reflection and fluorescence imaging. In the first case, the objective collects the light reflected by the sample. The resulting beam is then focused on the filtering pinhole before being picked up by the detector. The detection is therefore done at the wavelength of the laser emission. This technique has some advantages like the quantitative measurement of certain optical properties of the sample such as diffusion coefficients and reflectivity. It remains quite limited and mainly confined to the characterization of surface profiles or transparent multilayer samples. In the following section, we will

mainly address confocal fluorescence microscopy. This is a widely used technique that allows a wide variety of samples to be observed labeled or not. In this mode, the images are less noisy than in the reflection imaging mode. To fully understand the ins and outs, it is essential to recall some fundamental notions about fluorescence.

A molecule, whatever it is, has energy levels of different types (Figure 1.3a). In fact, a molecule is an assembly of atoms each composed of a nucleus (protons and neutrons) and an electron cloud. The interaction between the electrons of these atoms creates chemical bonds giving unity to the molecule. Each electronic configuration of the molecule confers to it a level of internal energy. The gap between these levels is of the order of a few eV. We can induce transitions between these levels using radiation in the UV visible range. Just as for the energy of the electrons constituting the molecule, the energy residing in the vibrational motions of the bonds is also quantified and gives rise within the electronic states to energy sub-levels. These vibrational states are much less energetic (5.10^{-2} eV) and can only be stimulated with infrared radiation. Similarly, within each vibrational state, there are different rotational states corresponding to different modes of rotation in the space of the molecule. The latter are even lower (10^{-5} eV). In general, transitions between the states mentioned above can take place, involving various modes of energy transfer. Our interest lying in fluorescence, we can conclude that the transition to a higher or lower electronic energy level can be achieved by the absorption or emission of a photon by the molecule.

In confocal microscopy, most often, a laser is used as a light source and is focused onto the sample. The photons of the incident beam can then interact with the components of the studied medium (molecules, ions, particles, etc.) and may be absorbed. Consider the case of a molecule. When it absorbs a photon, it goes from an energetically stable electronic configuration known as ground state (state S_0) to any excited electronic state. This event, called absorption, is characterized by two parameters, the wavelength of absorption (λ) and the probability that the photon will be absorbed by the molecule. The wavelength tells us the energy gap between the states brought into play in the process whilst the probability of absorption depends mainly upon the molar extinction coefficient (ε, $L.mol^{-1}.cm^{-1}$). This coefficient, widely used by chemists, is often replaced by the absorption cross-section of the molecule (σ, cm^2) by physicists or by the linear absorption coefficient (μ, cm^{-1}) in biology. Very simple relationships permit switching from one to

the other of these quantities. We can characterize, amongst others, a molecule by its absorption spectrum (intensity absorbed or absorption coefficient as a function of the wavelength) which is presented in the form of wide bands (Figure 1.3a) mainly owing to the different rotational and vibrational levels involved.

From the first moments following absorption, the molecule dissipates part of the energy supplied by the incident photon in relaxing itself vibrationally (internal conversion, IC) until reaching the excited electronic state lowest in energy (S_1). After a certain time, and therefore with a certain probability, the molecule loses the rest of its excess energy by radiation and relaxes toward a vibrationally excited state of the electronic ground state S_0. It emits a photon whose wavelength corresponds to this last loss of energy. This event is called spontaneous emission and the time spent by the molecule in the state of energy (S_1) is none other than the lifetime of this state, or the fluorescence lifetime (τ_F, s^{-1}). It can be measured in different ways, the simplest being following a prolonged illumination, then stopped, to calculate the exponential time decay constant of the fluorescence intensity collected. The fluorescence of a molecule can also be characterized by a fluorescence spectrum where the wavelength, as in the case of absorption, provides information on the energy gap between the levels involved and the intensity, on the probability of the event, therefore on the fluorescence lifetime. We can define, finally, a quantity called quantum yield (Φ_F) as the ratio between the number of fluorescence photons emitted and the number of photons absorbed by the molecule. This quantity depends upon the probability of non-radiative events, therefore upon their lifetime (τ_{NR}) and is inversely proportional to the fluorescence lifetime. Indeed, there are many ways for the atom to lose the excess energy that makes it unstable. It can transfer it to the environment in the form of heat or to another molecule through physical interaction, which will compete with the phenomenon of fluorescence and thus decrease its quantum yield [TUR 91]:

$$\Phi_F = \frac{\tau_{NR}}{\tau_{NR} + \tau_F} \qquad [1.28]$$

As the molecule has relaxed slightly vibrationally before emitting a photon, the fluorescence emission is always less energetic than the absorbed radiation. The emission wavelengths are always longer than the excitation wavelength. Moreover, as the structure of the S_1 electronic state is often

close to the S_0 state, their vibrational states are also close. We therefore most often observe a shift (called Stokes shift), an overlap and symmetry with respect to a centered wavelength between the absorption spectra and fluorescence spectra (Figure 1.3b). However, they differ almost always at least in their shoulders reflecting a slightly greater stability of one of the vibrational states of S_1 or S_0.

The phenomenon of fluorescence is made of incoherent and isotropic radiation. Also, unlike absorption, measured in the direction of the incident beam, it is often easier to collect the fluorescence at 90° from the excitation in order to not be blinded by it. In microscopy, owing to experimental constraints, it is difficult to be in such a configuration. Also, to separate the fluorescence emission from the incident beam, we detect the fluorescence emitted backwards (we call it epifluorescence microscopy) before performing a spectral discrimination based precisely on the Stokes shift, i.e. on the fact that the emission wavelengths are greater than the absorption wavelengths. We will see this in more detail later.

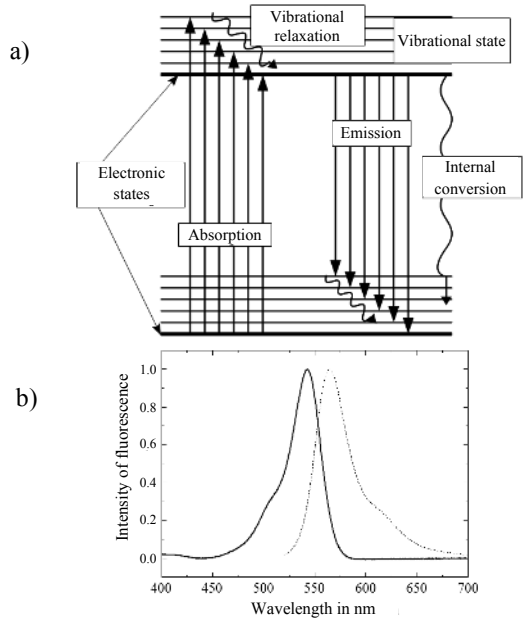

Figure 1.3. *a) Scheme of energy states involved in the process of fluorescence; b) example of absorption spectra (solid line) and emission spectra (dotted line) of a fluorescent compound*

It is important to note that not all molecules fluoresce; the ones likely to generate this kind of phenomena are called fluorophores, fluorescent molecules or fluorescent tag. There are many different kinds. Some are completely natural and already exist within living tissue. These are known as endogenous fluorophores. Others are completely synthetic and can label different types of tissues, cells and molecules. They are called exogenous fluorophores. Finally, a new class of fluorophores was discovered a few years ago, which can be placed on the border of these two large families. These are fusion proteins. This type of labeling involves fusioning a gene of interest with a known gene and coding for a fluorescent molecule. During the expression of the studied gene, a fluorescent graft will be added to the protein and this (the protein) can be followed throughout its path in the cell or the tissue studied. A more detailed description of these different types of fluorophore will be provided later, in the section on fluorescent tags.

1.2.4. *Main elements of a confocal scanning laser microscope*

We will now proceed to a slightly more detailed description of the key elements that constitute a system of confocal microscopy. This description will be done by following the path of the light, and therefore, will be detailed in the first place, the sources, then the dichroic systems allowing us to introduce an excitation beam within the device. We will also describe different scanning methods and their properties. We will focus on the objectives that are definitely at the heart of all microscopy, before finally ending with the solutions chosen to implement sensitive and resolved wavelength detection.

1.2.4.1. *Sources*

In confocal microscopy, the loss of the signal caused by filtering through a confocal pinhole requires the use of relatively intense light sources. The only solution lies in the use of continuous wave lasers (He-Ne, Kr, Ar) or diode lasers whose power varies typically from tens to hundreds of milliwatts. The illumination is therefore done with a coherent source, which will slightly affect image formation and greatly increase the cost of the system. Indeed, it generally requires a laser for each desired excitation wavelength. For this reason, Argon-ion lasers are very popular, since this technology provides access to ten wavelengths in the UV and 25 in the visible. However, for technical reasons and to avoid losing too much power, it is not possible to implement a laser of this type optimized for these

35 wavelengths! Only four wavelengths are available simultaneously in the violet and blue with the Argon-ion lasers of current confocal microscopy systems. Supplemented by the He-Ne lasers in the green, yellow or red, the range of excitation wavelengths becomes very interesting and covers the entire visible window with powers ranging from a few milliwatts to tens of milliwatts per laser line.

The use of incoherent illumination such as xenon short-arc discharge lamps (XBO) and mercury lamps (HBO), and light-emitting diodes (LED), is of little interest. Although they were used in the earliest developments, they have a spectral power which is too weak and, in particular, they do not allow a focusing power as localized as coherent sources such as lasers. They are however used in confocal microscopy systems with a spinning disk where extensive and uniform illumination is required.

1.2.4.2. *Dichroic elements*

To excite different fluorophores it is sometimes advisable or necessary to use different wavelengths (simultaneously or successively) and to be able to adjust their intensities independently. The most rudimentary confocal microscopy systems use a battery of interference filters mounted on wheels and coupled to filters of different optical densities. The first allows selecting one or more excitation wavelengths and the second, adapts their intensity to the observed sample. The disadvantage of this type of system is the slowness (of the order of seconds) of the mechanisms for changing filters.

Today, the most popular solution consists of using *an acousto-optic tunable filter* (AOTF). It is made of a somewhat special birefringent crystal (tellurium dioxide, for example) in which an acoustic wave propagates at high frequency, generated by a radio frequency electro-acoustic transducer. This acoustic wave generates, in the material, a refractive index grating able to deflect a narrow band of wavelengths in the first order. The deflected beam is then injected into the microscope. The number and relative intensity of the radio frequencies applied to the transducer allow the intensity and wavelength of the excitation to be controlled. In addition, it is possible with this type of system, to combine 10 to 12 independent channels making the excitation more flexible. Finally, the selection is faster, of the order of microseconds, significantly reducing the duration of experiments in sequential multi-wavelength confocal microscopy.

In confocal microscopy, excitation and detection go through the same objective because of the epifluorescence configuration, it is therefore necessary to use a system that allows us to inject the excitation beam into the objective and then to separate it from the emission after their return to the objective. The simplest system, still widely used, is to use a dichroic mirror. This element will act as a mirror by reflecting the excitation wavelength, then, at the return, as a filter to let pass only the emission wavelengths. The disadvantages of this technique are numerous; first of all, it is necessary to change the filter when the excitation wavelength changes. This requires the user to own quite a significant number of dichroic mirrors. Then, the spectral band of high reflection, which sends the incident light onto the sample, is relatively large (10 to 20 nm). It becomes quite difficult to correctly detect fluorescence at wavelengths close to the one used for excitation. In addition to working with several excitation wavelengths simultaneously, it is necessary to design multiband dichroic mirrors. This is not easy, or only at the cost of features that are even worse (in terms of bandwidths of rejection and transmission). Finally, these filters are placed in cubes inside turrets or wheels. The mechanism of changing filters is then a little fast, subject to wear problems and can cause errors of alignment.

It is possible to get rid of a lot of these problems by replacing the dichroic mirrors with an *acousto-optical beam splitter* (AOBS). The heart of this device is made of an AOTF arranged so that the laser excitation is coupled in the direction of the first order of diffraction. When returning, the fluorescence is transmitted in the order 0 without being affected, and the reflection of the excitation is deflected in the direction of the incident laser beam. The AOBS also includes a system allowing us to compensate for the birefringence and dispersion induced by the AOTF in the order 0. Its thinness, its effectiveness at rejection (2 nm > 99%) and its transmission (> 90%) make this type of system an ideal dichroic mirror. It usually has eight channels allowing the injection of, simultaneously or not, eight different laser lines, which is equivalent to 255 dichroic mirrors! In addition, the tunability of wavelengths controlled by a simple change of frequency can be done very quickly and allows, as with the AOTF, a non-negligible saving of time during sequential experiments. Finally, the AOBS can be programmed by the user, which gives this device unlimited flexibility. It allows us, for example, to carry out within the same image, an illumination of different regions at different wavelengths.

We last recall that, during experiments of reflection contrast microscopy, a simple semi-reflecting mirror is sufficient, since the detected wavelength is the same as the incident wavelength.

1.2.4.3. *Scanners*

In confocal laser scanning microscopy, we saw that we acquire the fluorescence or reflection from a single point. In order to reconstruct an image (indeed a volume) it is necessary to be able to shift the focal volume transversely in the object plane, indeed, shift it axially. There are a few solutions for this that we will outline below.

The simplest solution is to leave the beam fixed and to only translate, perpendicularly to the optical axis, the stage on which the sample is positioned. This kind of system is based upon the use of simple motorized stages with step motors or the use of piezoelectric technology for faster scanning. If the sample cannot easily be moved, there are similar systems where the scanning is performed by moving the objective, which can be problematic when using large objectives. In addition, in the latter setup, the beam does not necessarily fulfill the rear pupil of the objective and problems of loss of intensity in the corners of the image (vignetting) and loss of resolution can be observed. Displacement of the sample can also cause some problems because the speeds reached by the scanners, corresponding to the sampling frequency, are not as important as the ones obtained through devices which will be discussed later. However, it allows limiting certain optical aberrations since the beam always remains aligned along the optical axis. It may therefore be useful when using very specific objectives, or when the scanning speed is not crucial.

The most used solution in confocal laser scanning microscopy consists of placing an optical scanner between the objective and the dichroic element to allow the beam to be “descanned” and to ensure that the probe point is always conjugated with the confocal pinhole. This scanner is usually composed of two mirrors oscillating at high speed and driven by galvanometric motors. These mirrors oscillate along two perpendicular axes and therefore allow sweeping the entire sample. There are also configurations where only one mirror oscillates in both directions. One of the two axes is scanned by a very fast motor to allow acquisition of a line of spots, whilst the other can be scanned more slowly to move this line and reconstruct the image. These scanners offer many configurations and have

undergone enormous developments to meet certain criteria. First, to avoid suffering loss of intensity during illumination and to make the most of the resolution of the equipment, it is always necessary that the beam exactly fulfills the rear pupil of the objective throughout the whole scanning cycle. One of the solutions used to solve this type of problem is to rotate the beam around a fixed point of a plane conjugate to the entrance pupil of the objective. It also requires that the scanner minimizes the dead time, i.e. the times when the beam arrives at the sample without any signal being recorded (end of line or between two images). This allows both a backup of the sample and a possibility to increase the illumination and therefore to achieve a better signal to noise ratio. The implementation of these galvanometer scanners is now very well understood by manufacturers and offers many advantages. By changing the angular range scanned by the mirror, you can zoom in on the sample from × 0.6 to × 100 and even sometimes × 1,000. In addition, the sampling frequency and size of images can be easily adjusted (from hundreds of Hz to about 5,000 Hz, and from a single point to 4,096 × 4,096 pixels per image).

The biggest problem of this type of system lies in the optimization of the scanning speed. Although the galvanometer mirrors can oscillate at relatively high speeds, this type of scanner unfortunately does not allow us to reach video speeds. However, this issue is crucial for monitoring fast biological phenomena. It is very difficult to exceed eight frames per second (512 × 512 pixels). Indeed, during scanning, the rotational speed of the mirror must be constant so that the illumination stays homogeneous on a given line. However, this involves, at the beginning and at the end of a line, a sudden change of direction for the mirrors. This velocity discontinuity will be more violent if the scanning frequency is high and it is therefore this phenomenon that limits the scanning frequency to prevent damage to the system.

The slowness of this type of system is mainly owing to the inertia of the mirror scanning the line or to the fast mirror. One technique consists of vibrating the mirror sinusoidally to avoid discontinuities of the velocities. The frequency used can reach 8,000 Hz, an imaging of 16,000 lines per second by recording the signal going and returning (about thirty frames per second at 512 × 512). As the signal is recorded without taking account of the velocity variation of the mirror, two important problems occur. First, the sample is scanned faster (maximum speed of the mirror) at the center of the image than at the edges (null speed of the mirror). This creates a distortion of

the image which is compressed at the edges. Fortunately, this distortion can be corrected either by modeling the mirror oscillation or by directly following its movement by an optical method. Another disadvantage is that the sample undergoes a prolonged illumination at the beginning and at the end of a line inducing risks of non-uniform photobleaching. With this technique, some of the maneuverability of galvanometer scanners is maintained. In particular there is the possibility of zooming up to × 8 or adjusting the size and definition of the image to again increase the frequency. This is not the case with the methods we will see later.

Other approaches have been developed to improve the sampling frequency. Among them, one solution is to shape a line of illumination to simultaneously record the signal on one axis and to scan in only one direction. Then the galvanometer mirror used does not need to be too fast, and the scanner system is cheaper. This technique also allows us to increase the time spent by the laser to illuminate each pixel of the image. The detection is no longer done by a confocal pinhole and a photomultiplier, but by a slit and an aligned CCD (Charge-Coupled Device) camera. The big disadvantage of this technique is that the resolution is no longer symmetrical. It corresponds to a type of confocal resolution on the axis swept by the mirror and filtered through the slit, and to a type of classical resolution (wide-field) on the axis corresponding to the slit or the line of illumination. In addition, the use of a line does not provide a resolution as well as with a point, which makes this setup rarely used. However, owing to their speed of acquisition, these methods have been experiencing somewhat of a revival since the arrival of high sensitivity cameras such as the Electron Multiplying Charge-Coupled Device (EMCCD), Intensified CCD (ICCD) or Complementary Metal-Oxide-Semiconductor (CMOS) making detection much more sensitive than with the CCD line. These two-dimensional detectors allow us, in addition, to glimpse the possibility of both a spatial and spectral resolution.

To perform a scan, some devices use a type of acousto-optic deflector used for injecting the beam into the microscope. Indeed, this component can diffract or refract a light wave with an angle dependent on the frequency of the acoustic wave passing through it. We can therefore, by scanning the correct frequency range, move the focal volume inside the plane of the sample. This system has the advantage of coming almost instantaneously to the beginning of the line and can be programmed by the user. The disadvantage is that it is based upon the dispersive properties of the material

used and is therefore set for a single wavelength. It is difficult to "descan" the fluorescence if it comes in the form of broad spectral bands. So a slit rather than a confocal pinhole must be used and the axial resolution is thereby reduced automatically. Although promising, this type of device is rather ignored by manufacturers.

There are also some microscopes that use a spinning polygon in order to scan the sample. The beam reflects on one side, and then the spinning of the polygon generates a rotation of the face and therefore a deflection of the beam. The same deflection then occurs on the next face and so on. This method seems simple, but is proving rather difficult to implement. This system is very sensitive to small variations in reflectivity and angle. It is therefore necessary to add a system of optical correction which can be complex. Another constraint is that the number of faces that can be designed as a polygon is not unlimited (15 to 75). The number of lines per second is a multiple of the number of faces of the polygon and its speed must be very high to reach video frequency (respectively 63,000 to 12,600 rpm). It is therefore necessary to provide a robust support and the vibrations should be reduced. All these minor inconveniences prevent this kind of device being more widely used by manufacturers now. It is found in specific applications where high speed scanning is required.

Generally, we must not forget that the more complex the optical system is in the scanner, the more it will decrease the luminosity of the device. The compromise between speed, transmission and accuracy is important, and will essentially depend upon the application.

In this chapter, we will focus only on confocal laser scanning microscopy. We will not deal with other types of confocal microscopy. They are based upon the idea of illuminating the sample at multiple points simultaneously and then detecting the signal sent to a camera (CCD, CMOS, EMCCD, etc.). For this, it is necessary to expand the beam to split it up through an optical system. This device is at the heart of the technique and gives its name in general. This may be a spinning disk drilled with a great number of pinholes (Nipkow disk) or a spatial light modulator such as the array of programmable micromirrors (APM). A light signal (fluorescence or reflection) is returned by each illuminated point and returns to the previous system to be filtered which gives to this microscopy a confocal character. This type of device is not very bright, but can achieve noteworthy frame

rates thanks to the simultaneous measurement (up to 2,000 frames per second).

To finish, we need also to put in place a scan of the sample along the optical axis, if we want to achieve stacks of images. This last point is much less important since it is not limiting, both in terms of speed and luminosity. It is most often carried out by a step motor with a feedback loop system for the position in order to vary the distance between the objective and the sample (either by moving the objective or the stage carrying the sample). Most manufacturers offer solutions allowing a minimum displacement of about 10 nm, which is well below the resolution or the thickness of the optical section (see the section on resolution). In addition, there are overstage or shim objectives equipped with galvanometric motors or piezoelectric wedges. These systems achieve a longitudinal scanning of the sample (or the objective) at high speed. Accordingly, by scanning the beam on one line, and by combining a scan along the optical axis with these systems, it is possible to take images in a plane containing the optical axis. This type of scan can be interesting if you want to measure roughness profiles or study multilayer media. These systems can vibrate at rates of the order of several hundred to a few thousand hertz. The path scanned can reach the order of millimeters and the accuracy of positioning can reach the nanometer scale. However, these characteristics depend upon the technology chosen and are also interdependent (e.g. if the range is significant, the frequency must be reduced, as for optical scanners). Again, it is the application that will determine which features to choose.

1.2.4.4. *Objectives*

Once scanned, the beam enters the objective and focuses itself on the sample, generating a fluorescence emission, a little reflection and backscattering. This light is collected by the objective and again follows the path we have described in the opposite direction up to the dichroic element. The objective is at the heart of a microscopy setup and is certainly one of the most important elements. Contrast, resolution, imaging depth and the field of view are the features upon which the objective will have an important influence. It is the objective which, by its diffraction, will limit the resolution of the setup (see resolution). This is the element which is often changed and which eventually will adapt our system to the desired study. There are as many kinds of objective as types of microscopy. Finally, this element is

particularly important in confocal microscopy as we seek to work with a very high resolution and with very few photons.

It is obvious that in fluorescence contrast confocal microscopy, the objective must not fluoresce. In addition, for applications in UV, optics must be composed of fused silica or quartz. For near-infrared applications, the objective must be sufficiently transparent so that the power of the beam or of the fluorescence is not too attenuated. It is therefore necessary that the anti-reflection treatments of optics are very good. Today, most manufacturers offer objectives whose transmission is greater than 50% in the area 350-1,000 nm. There are also specialized objectives in the UV visible, and others in the near infrared (for nonlinear microscopy, for example).

The three features which are the most important to take into account, those of which we speak most often to describe an objective and which are recorded on it, are certainly the magnification, numerical aperture and immersion medium. These three characteristics are somewhat related. The numerical aperture, for example, increases with the index of the immersion medium and, in general, the magnification. Indeed, the larger the latter, the smaller the working distance and the larger the acceptance angle of the photons. However, the numerical aperture becomes $\mathrm{NA} = \mathrm{n}\sin(\theta_0)$, thus, if the maximum angle of entry or the index of the immersion medium increases, the aperture also increases. However, this trend is not systematic, since there are ×20 objectives with high numerical apertures (up to 1) and ×60 objectives with numerical apertures less than 0.8. The magnification of an objective can take extreme values. Manufacturers offer systems that can magnify from 1.25 up to 150. Immersion media, meanwhile, are becoming increasingly diverse. The most common are air (“dry” objective), water and oil, but new optics have recently been optimized to work in media such as glycerol or silicone oil, which are better suited to the refractive index of biological media. Note, however, that there are objectives with an adjustment ring allowing selection of the desired immersion medium. Finally, the numerical aperture, depending largely upon the two previous parameters, can drop very low for macro objectives (× 1, NA = 0.035) and can go up to nearly 1.5 (which corresponds to a light collection in a solid angle of nearly 2π steradians). It is essential to choose the right objective for the type of experience you want. In fact, for numerical apertures which are too low, it is not impossible that, in the case of rather thin samples, the axial resolution is greater than the thickness of the observed object. In this case,

we cannot really speak of a confocal technique. Indeed observing a slice of 10 microns with an objective opening at 0.2 (resolution ~ 12.8 microns) does not really make sense in confocal microscopy because the axial resolution is then greater than the thickness of the sample.

Most often, it is aberrations which limit the performance of the objective. We will not cover here a full course on aberrations, but understand the principle and grasp the impact they might have on imaging in confocal microscopy. For more details, there is relatively extensive literature on the subject [BEC 06]. Different types of aberration tend to distort the image or reduce its intensity, especially as for high numerical aperture objectives, the angles of extreme beams can become very large and the paraxial approximation becomes less and less justified. These aberrations can be divided into two groups. Firstly, there are the geometric aberrations which are not dependent on the wavelength of the radiation. The most important is undoubtedly the spherical aberration. It follows from the properties of spherical lenses for which paraxial and peripheral rays do not focus in the same plane. This phenomenon is usually accounted for by particular designs of optics to the point that it becomes negligible compared with diffraction.

Objectives are subject to other types of geometric aberration such as coma, field curvature, distortion and astigmatism. When an objective is supposed to be corrected for spherical aberrations, it is also done for all these geometric aberrations. In addition, the objective is subject to chromatic aberration which, as its name suggests, is a phenomenon depending upon the wavelength. Optics of objectives are built of dispersive materials for which the index of refraction varies with wavelength. The shorter the wavelength of the considered radiation, the closer its focal point will be to the objective. This is what is called the axial chromatic aberration or aberration of chromatic position. If the focal lengths are different for two light beams, we can deduce that the magnifications are also different. There then appears a second type of aberration which becomes stronger as we move away from the optical axis. In this case, the longer the wavelength, the further from the optical axis the focus point will be. For this reason, these aberrations are called lateral chromatic aberrations. In confocal microscopy, chromatic aberrations are particularly troublesome. Indeed, the excitation and emission wavelengths are very different, it is therefore necessary to be sure to work at the same depth regardless of the radiation. In addition, if for example we look to verify the co-localization of two fluorophores of different colors in a single image, the lateral chromatic aberration is then prohibitive.

The objectives are grouped into different categories corresponding to the degree of correction they possess. Firstly there are *achromatic* objectives, having a slight correction for chromatic aberrations and *plan achromatic* objectives having, in addition, a basic correction for spherical aberrations. Then comes a fairly recent series containing fluorite elements or materials in which the dispersion is close to it, and which displays much more drastic correction for chromatic and spherical aberrations. These objectives have the added advantage of having good correction in the UV. They are grouped under various names (*Fluor, FL, FL Neo, semi apo*, etc.) and represent a good compromise between correction quality and price. Finally, the objectives listed under the name *apochromatic* have the highest level of correction. They have, moreover, a greater numerical aperture for a given magnification. They are much more expensive, but are especially recommended for confocal microscopy.

It is as well to remember that an objective is designed to work for a certain distance, with a well-defined immersion medium, and for a type of sample that is well suited to the immersion medium. Most optics are made to work with a single type of microscope coverslip whose size is variable (0.13 to 0.21 mm). Several objectives have been designed to meet some of the expectations of biologists and can work in immersion, i.e. by placing them directly against the medium to be observed. They are particularly suited to work on living biological material (and thus mainly composed of water, unlike the attached biological material). Finally, some have an adapter ring allowing us either to adjust the working distance, to accommodate the size of the coverslip used, or even to select the type of immersion medium.

It is necessary to bear in mind when working in confocal microscopy that the characteristics of the objectives are set by the manufacturers and therefore can be used only for a specific application. Any use of the objective outside the conditions specified by the manufacturer will automatically cause an increase in chromatic and spherical aberrations which can lead to a degradation of the resolution and a possible alteration of the image (integrity of the axial or lateral resolution) and a loss of contrast and intensity. Failure to comply with the optimal conditions for using an objective can come from a poor choice of immersion medium, irregularities in or the wrong thickness of the coverslip, a setup not suitable for the immersion medium, or the sample itself. In fact, in the case of high-magnification or high numerical aperture objectives, aberrations can only be perfectly corrected by a very special positioning of the object plane. The

image of this plane by the objective is then without aberration and, in general, suppliers arrange for it to be about 15 or 20 microns under the coverslip.

We have finally seen that there are a lot of objectives, almost as many as possible applications. Choosing the right tool is essential. Which area of the sample we would like to look at, with what accuracy and what this sample is mostly composed of are essential questions to ask when you set up an experiment in confocal microscopy.

1.2.4.5. *Detection systems and spectral resolution*

For each point scanned, it is now necessary to measure the fluorescence signal or the reflection signal collected by the objective. The easiest way is, of course, by placing a detector just after the confocal hole, then measuring the intensity of the light passing through it. However, most often, the equipment of confocal microscopy shows a spectral detection window allowing the separation of various fluorophores and making images with several "colors" in several measurement channels. Two parts must be distinguished in the detection, one allowing us to separate the beam spectrally, and the other measuring the intensity of radiation in different wavelength bands.

At the exit of the hole, the beam first passes through a lens whose object focal plane is located at the diaphragm for collimating the beam. Then, different layouts exist, that depend mainly on manufacturers. The simplest is to have a wheel containing a battery of bandpass filters (5 to 20 nm wide) and to record images successively at different wavelengths. Using a set of suitable dichroic mirrors and filters, it is possible to record several spectral bands simultaneously.

Another solution is to perform a spectral decomposition of the beam through a dispersive system in order to record several spectral bands emitted by the sample simultaneously. Two configurations are then possible. The beam is dispersed by a prism and part of the spectrum is selected by a mirror slit of variable width. Wavelengths crossing through this slot are collected on a photomultiplier whilst those reflected can be sent to another slit-photomultiplier module. Adjustment of the position and width of the slit is used to select the center and width of the spectral range of interest. However, to measure several bands simultaneously, it is then necessary to have as many channels measured as fluorescent molecules. If the number of channels

is too low, we have to go back to an alternative acquisition mode, which increases the acquisition time.

Another solution is to diffract the beam by passing it (several times) through a diffraction grating and recording the spectral signal through a multichannel detector (up to 32 channels in some manufacturers). Feedback controls on the grating and on the leading mirrors of the grating allow us to send any part of the spectrum to the detector. The resolution of the device depends upon the detector's pixel size and upon the diffraction grating. For this reason, we often find in this kind of device a turret containing different gratings to better adapt the detection to the experiment. This technique has the major advantage of recording 30 images at different wavelengths simultaneously. This almost gives an emission spectrum of the sample.

Finally, there remains the choice of a suitable detector for confocal microscopy. This choice may, for example, be based upon the spectral range to be used and on the average quantum yield which can be achieved in this range. These two values together allow us to know, for a given wavelength, the ability of our detector to provide an electrical charge in response to the arrival of a photon. It is also important to know the spatial resolution of the component and its uniformity, i.e. its response as a function of where the photon hits. Another key feature is the signal-to-noise ratio. It takes into account the stochastic noise inherent to a stream of photons, the noise of the measurement equipment following detection (readout noise) as well as the intrinsic noise of the detector when it receives no signal (dark noise). The dark noise is strongly dependent on temperature and can vary widely from one detector to another. Finally, it is important to use an instrument with a dynamic adapted to our measurement. This value corresponds to the gap between the lowest and highest measured signal. Finally, depending upon the application, for monitoring biological mechanisms for example, it is essential to focus on the response time of the detector. This latter characteristic is even more critical in certain specific applications, such as the measurement of fluorescence lifetime (FLIM technique, described later).

In the case of confocal laser scanning microscopy, the different points of an image are observed sequentially (due to scanning); it is not useful to have a detector with a spatial resolution. However, it is essential to use a very sensitive system since much of the radiation is stopped by the confocal pinhole and the fluorescence itself is often quite weak. In addition, the

detector must have a relatively short response time so as not to limit the rate of imaging.

The possibilities are essentially limited to two types of component: photomultipliers (PMT, *Photomultiplier Tubes*) and *avalanche photodiodes* (APD). PMTs are the most widely used; they are composed of a quartz tube under vacuum containing a photosensitive surface. This area, called the photocathode, generates electrons by the photoelectric effect when struck by photons. These electrons are accelerated toward an electron multiplier composed of a sequence of arc-shaped dynodes, each one amplifying the signal originally emitted by the photocathode. The electric circuit ends at an anode, from which exits a current proportional to the number of photons hitting the entrance face of the detector. The critical element, the photocathode may be composed of alkali metal (most commonly) providing a quantum yield of about 20% for the visible range. New detectors made of a semiconductor photocathode (GaAsP) achieve quantum yields of about 40% between 300 and 700 nm. They can be quite noisy and require a cooling system like Peltier. The photocathode reacts instantly to the incident light flux, there is therefore no accumulation of charge. Also, the response time of this kind of detector is very fast, in the order of nanoseconds. The alkaline-type PMT has the big advantage of having a relatively low noise and therefore has a very good dynamic. In addition, the opportunity to work with an unparalleled gain (about 10^7) allows a relatively high signal-to-noise ratio to be achieved whilst keeping a good sampling frequency. The weak point of this type of system lies in the uniformity of the photocathode, it is preferable to ensure that the beam covers the entire front face of the detector rather than a small part of it. It is worth noting that within the same production line, disparities in the gain and dark noise can reach factors ranging from 2 to 5. These systems are relatively sensitive to the incident flux and can easily be damaged by too much light.

Recently, avalanche photodiodes, from silicon photodiodes, made their appearance in confocal microscopy. Their operating principle is similar to that of classical photodiodes. APD silicon is thus made of three types of PIN semiconductor layer, a P-doped layer and an N-doped layer, separated by a depletion layer. When a light beam strikes the photodiode, and its energy is greater than the forbidden band gap, an electron-hole pair is created in the depletion region. When the electron-hole pair, which plays the role of charge carrier in this type of material, is created and a current is applied to the PN junction, the electrons migrate to the N layer (which is negatively charged)

and the holes to the P layer (which is positively charged). If we apply to the PN junction a reverse voltage close to the breakdown voltage, the energy of the carriers can then be sufficient to create other carriers in the crystal by collision. This is what is called the avalanche phenomenon. APDs are very sensitive and the combination of their gain (up to 300) and their good quantum efficiency (>70%) allows them to operate in photon counting. Unfortunately, they are very sensitive to the shot and dark noise which will, moreover, be amplified by the gain. They should therefore be used at low temperatures. Whilst photomultipliers are the most popular, some manufacturers offer a measurement using APD for storing images of samples emitting a low number of photons.

We saw earlier that for certain types of spectrum detection, it is necessary to use a multichannel detector. Recently, some manufacturers have put on the market multi-anode PMT (type GaAsP). In this type of system, the special configuration of the photocathode and anode allows us to retain spatial information on the detected photon. Designers of confocal microscopes now incorporate devices in line counting up to 32 channels offering the ability to perform 32 simultaneous spectral images of the sample. Other manufacturers have followed a similar path leading to the development of arrays of silicon APD. The difficulty of such systems lies in the miniaturization of components.

Finally, we have seen that some experimental devices (line scanning microscopy, spinning disk) required the use of classical or aligned cameras. Among the most popular are obviously the CCD (*Charge-Coupled Device*), which has recently been supplanted by EMCCD (*Electron Multiplying CCD*) type cameras and ICCD (*Intensified CCD*), in applications requiring the highest sensitivity. A CCD camera is simply a matrix of photodiodes incorporating a charge storage area. Each photosite or each pixel is capable of converting photons hitting it into electrons and accumulating them in a potential well. When exposure time is completed, the charge stored in the last row of pixels is shifted to a line register and then read by an amplifier and digitized by an analog/digital converter. The remaining lines of pixels are then shifted parallel to the line of the register to be read one after the other. CCD cameras are quite prone to readout noise caused largely by analog amplification which makes them inefficient for the detection of weak signals. In the early 2000s, manufacturers were able to develop a type of camera based upon the same kind of technology but much more sensitive, the EMCCD. The principle is quite similar, although an essential step is

added before reading the amplifier. After transiting via the readout register, the electrical charge is moved to a register called a "multiplier" consisting of an electron multiplier. They are then read by the amplifier and digitized. This process is extremely valuable as it allows weak signals (gain of about 300) to be amplified before they are affected by most of the readout noise. This allows this camera to operate in photon counting which has led to a renewed interest in multibeam systems and enabled the achievement of single particle imaging. Finally, a further type of camera based upon CCD technology has recently appeared, ICCD cameras. They have a light intensifier coupled to a CCD sensor with low readout noise. Incident photons arrive at a photocathode (most often GaAs) and generate electrons, which will be amplified by a microchannel plate. These electrons then bombard a fluorescent screen imaged onto the CCD sensor. The advantage of this type of system is that the intensifier can be closed very rapidly and the exposure time can be reduced to less than 80 ps. The low quantum efficiency of the photocathode (<50%) unfortunately makes them less sensitive than EMCCD and does not allow the detection of single photons.

1.3. Applications in biology, potential and limitations

As we saw in the previous section, confocal microscopy offers, at least on paper, a tremendous potential for imaging with, on the one hand, a resolution at the limit of what an optical method can provide and, on the other hand, an axial resolution allowing either an extension of the depth of field or a three-dimensional reconstruction. However, the previous section also provided a glimpse into the technological complexity required for the implementation of this imaging method. This complexity makes this tool quite expensive and requires qualified personnel. In addition, a biologist used to wide-field fluorescence microscopy may sometimes be disappointed by the quality of the images obtained by confocal microscopy. Indeed, it would be naive to think that confocal microscopy is a better method and thus makes others obsolete. Certainly, it is a major breakthrough in optical microscopy offering a higher resolution (especially axial), but this can be at the expense of other performances. In this section, we will discuss the implementation of confocal microscopy in biological samples and we will attempt to provide a critical point of view and highlight some limitations and artifacts.

1.3.1. *Basic elements of biology for the neophyte*

To understand the applications, advantages and limitations of confocal laser scanning microscopy, it is necessary to talk a bit about biology. The reader will quickly (especially if he/she is a biologist!) see that this section is not very ambitious, even sometimes almost voluntarily naive. Its purpose is simply to give a bit of technical knowledge on the basic elements of cellular biology because it is at this scale (the scale of the cell) that confocal microscopy reveals all of its potential.

As everyone knows, at the microscopic level, life is composed of a set of cells whose sizes, shapes and especially *functions* within the same organism may be very different. The prokaryotic cell (bacteria) has no nucleus and typically measures between 1 and 10 microns. The eukaryotic cell (animals, plants, fungi) has a nucleus and can typically measure between 10 and 100 microns. Each cell is bounded by a hydrophobic lipid membrane called a plasma membrane. On this membrane are inserted many molecules, especially proteins, which will allow either the outward transit of molecules synthesized by the cell, or allow the entry of other molecules, or "probe" the extracellular environment (presence of hormones, etc.) and trigger a whole series of reactions accordingly (we therefore speak of membrane receptors). Inside the membrane, we find the cytosol, an essentially aqueous medium in which bathe sub-structures called organelles. These organelles are themselves bounded by lipid membranes. These include for example:

– the nucleus, which contains the DNA of the cell;

– the mitochondria, in which is synthesized the adenosine triphosphate (ATP) which is used to provide energy to the cell;

– the endoplasmic reticulum, which participates in the transformation of proteins synthesized by the cell and in the synthesis of lipids;

– the Golgi apparatus, which is also used for the transformation of proteins and transiting them towards the outside of the cell, in particular.

To this list, although it is not exhaustive, we add the lysosomes, endosomes, peroxisomes, etc., or yet more organelles specific to a cell type, such as the chloroplasts of plant cells for example in which photosynthesis occurs. Finally, the cell has a cytoskeleton, made up of different fibers, flexible (actin filament) or more rigid (microtubules) which have diameters

of the order of a few nanometers (between 5 and 25 nm according to their type). This cytoskeleton allows the cell itself to deform, to spread, to hold or to move and plays an important role in the smooth functioning of cell division (mitosis).

In addition, you should know that biological tissue can be composed of an assemblage of juxtaposed cells (called epithelium), but more often, the cells are embedded in an extracellular matrix (called connective tissue). This is the case for example with the skin, made up of a dense and fibrous extracellular matrix in which we find proteins and glycoproteins such as collagen. Cartilages and bones are also good examples of connective tissue. In the case of bone, in addition to collagen, the extracellular matrix is composed of crystals to ensure its strength. Finally, with a few rare exceptions, these different animal tissues are covered with a more or less dense network of blood vessels and nerves that circulate oxygen, nutrients and chemical or electrical information.

In this great variety of microscopic tissue structuring, then sub-structuring within the same cell and the huge amount of chemical reactions that take place, the biologist seeks to understand the roles of different cells, the roles of different cellular organelles, different proteins and different parts of the genome, and tries to decipher the communication between cells and the cascades of reactions that can be triggered. That is to understand, for example, how a cell decides to destroy itself (apoptosis) during the development of an organism; why an organ or group of cells will no longer perform their duties in the case of pathologies; by what means, with which treatment we can destroy a tumor; by which mechanism a virus will infect a cell; how, during development, a stem cell will suddenly be agitated by a cascade of chemical reactions that will finally trigger differentiation. To understand life with such a level of detail, classical optical microscopy is not sufficient to explore the biological and biochemical mechanisms. Indeed, the study of the structure of single cells and tissues does not allow us to comprehend the complexity of the functions and mechanisms of cellular function.

On the other hand, fluorescence confocal microscopy offers a better contrast and the possibility of virtual slicing of the sample. This is an important step towards a more accurate and especially three-dimensional study of the distribution of macromolecules (proteins, membrane receptors, cytoskeletal fibers, etc.,) within a cell or an organelle. Furthermore, confocal

microscopy provides a tool to work on thicker samples by reducing the disturbance caused by stray light coming from blurred areas. This allows envisaging work on living cells or tissues, or in any case, on thicker slices, which limits the possibility of damage to more fragile tissues. Finally, the coupling of the confocal microscope with fluorescent tagging samples (see next section) provides the possibility of localizing a molecule with great specificity, a membrane receptor or a given organelle. In other words, fluorescent labeling has the potential to make luminous, in varying ranges of color, one or more types of molecule, one type of membrane receptor, one type of organelle, a virus, a bacteria and to then study their absence/presence, concentration, three-dimensional distribution or even their co-localization, which may be a clue to molecular interaction.

1.3.2. *Fluorescent labeling*

Sample preparation and, in particular, the labeling of structures or specific molecules is a key step for observation in fluorescence microscopy. Molecules and fluorescent objects and tagging techniques represent a broad topic and we will attempt here to give a representative overview of the many possibilities that are available. For more information, the reader is referred to more complete works [PRA 03] or to the many documents and handbooks of manufacturers of fluorescent probes.

It makes sense to start by talking about endogenous fluorescent substances, i.e. fluorescent molecules naturally present in an organism. These molecules are not necessarily very strongly fluorescent, nor necessarily very specific, but they may be of interest in minimally invasive *in vivo* studies. For example, plants are composed of many organic molecules, some of which have a very strong fluorescence, especially under UV excitation. The most obvious example concerns chlorophyll which fluoresces in green and red under UV excitation. In animal biology, prime examples are nicotinamide adenine dinucleotide (NADH) and flavins, molecules heavily involved in the regeneration of ATP (adenosine triphosphate) and therefore in the mechanism of energy consumption of cells. During the consumption of energy, these substances are oxidized, thereby changing their fluorescence. The endogenous fluorescence of tissues can then be used as a monitoring method for oxidation and therefore of energy consumption [MAY 07].

Beside these special cases of endogenous fluorescence, it is necessary to introduce exogenous fluorescent substances to achieve fluorescent labeling of tissues or cells for observation by confocal microscopy. The first idea, inspired by what had already been done in bright-field optical microscopy (staining), relies upon the creation of a simple tag using fluorescent molecules that have a particular affinity for a molecule of biological interest (through a chemical bond, an intercalation or a simple selective miscibility). In this category, there is a multitude of molecules able, for example, to intercalate themselves in the DNA (DAPI) or to fit into the cell membranes, mitochondria or endoplasmic reticulum through their carbon chains and their affinity for lipids (carbocyanines).

To extend the range of possible fluorescent tags, but with increased efficiency and specificity, another method is immunofluorescence labeling. This method involves using antibodies, i.e. proteins used by the immune system to detect and disable another specific protein (typically) thanks to a very specific attachment. The most flexible protocol is to proceed in two steps, indirectly: we synthesize an antibody (called primary) that on one side is capable of binding specifically to a macromolecule of interest and on the other side allows the attachment of another antibody (called secondary), previously bound to a fluorescent molecule. The very broad possibilities and specificity of such a labeling make them a now widely used method in fluorescence microscopy. A wide range of commercial antibodies can be found, labeled with the help of organic molecules which are stable and highly fluorescent (Alexa Fluor series, for example, with fluorescence available from blue to near infrared). Recently, antibodies labeled with semiconductor nanocrystals called *quantum dots* have also appeared, whose luminescence is very high and very resistant to the laser flux. In addition, these nanoparticles have a relatively narrow emission spectrum that can reduce the risk of spectral overlaps of different fluorescent tags in multiple labelings.

Another technique for labeling which is even more subtle and advanced[2] consists of using a fluorescent fusion protein, of which the most well known is the GFP (*Green Fluorescent Protein*) [TSI 98]. There is now a wide range of fluorescent proteins emitting bands of various colors. The technique of

2 In order to understand the considerable advance that this technique represented for biology, it is interesting to note that the discovery and development of GFP earned the 2008 Nobel Prize for Osamu Shimomura, Martin Chalfie and Roger Y. Tsien.

labeling by fusion is a technique of genetic engineering which consists of modifying the genome of an organism or cell by inserting a gene responsible for the synthesis of a fluorescent protein. This type of labeling is not easy to achieve and requires a number of advanced tools and methods of molecular biology. However, this method of labeling is very powerful because it allows us to label non-invasively a living organism (or rather to create an organism that expresses a fluorescent tag) with a non-toxic molecule that does not alter its physiology. Depending upon how we proceed, the labeling may be expressed in a certain type of cell or in certain cell compartments and not in others. It is an interesting tool in developmental biology, for example, because it allows us to track the expression of a particular gene in the development of an animal [CHA 94].

The three main categories of fluorescent tags and labeling techniques mentioned above do not reflect all the possibilities and all the subtleties that can provide fluorescent labeling. Based upon the very advanced knowledge that we have today on the interaction between light and molecules, several fluorescent probes can indirectly provide more than just location. Indeed, some fluorescent molecules are very sensitive to their environment (pH, solvent polarity, binding, etc.). Consequently, their fluorescence can be altered and cause modifications independent of their concentration (via the quantum yield, the absorption spectrum or the emission spectrum). This principle is the basis of ratiometric probes (FURA-2, INDO-1, etc.). This type of probe can monitor the concentration of the substance to which it is sensitive by studying the ratio between two levels of fluorescence measured for two different excitation wavelengths. Other types of interaction affecting the fluorescence are at the origin of FRET (*Fluorescence/Förster Resonance Energy Transfer*) to detect, for example, if two proteins interact. This technique is based upon the use of two fluorescent molecules whose properties are selected so that, in the absence of interaction, and for a given excitation, one fluoresces well in a certain spectral band and the other very little and in another band. Once in contact, the first is capable of transferring the absorbed energy to the second which begins to emit more fluorescence.

To finish, we will focus on the limitations that should be taken into account when choosing a fluorescent tag and a type of labeling technique. Concerning the physical and technical limitations set by confocal microscopy, it is necessary to use molecules which are highly fluorescent, i.e. very absorbent, but which also have a strong fluorescence quantum yield.

This will be especially true if the labeled sites are rare and diluted and if we seek the ultimate resolution of confocal microscopy. Indeed, in such cases, the volumes probed by the focused beam constitute a fraction of a femtoliter, which only represents relatively few molecules! In addition, the need to use a high power laser beam implies using very stable molecules, i.e. not prone to photobleaching. Finally, it will be necessary to select fluorophores with absorption bands corresponding to the available laser wavelengths. In addition to these considerations related to imaging technique, there are many other limitations related to the biological question and the sample. Indeed, the relevance of a given fluorescent tag will depend upon whether or not it is necessary to work on a live sample (cell, tissue, organ or organism). In this case, it is necessary that the fluorescent probe is not toxic and does not alter (or does not need to alter) the proper functioning of cells. For example, immunostaining is, most of the time, impossible because the penetration of antibodies into the cell requires piercing the membrane with detergents. The large size of the antibody also limits the penetration of the fluorescent tag and makes it difficult to label in tissue to more than 50 microns, typically. However, specific *in vivo* labels are possible thanks to GFP, for example. An *in vivo* labeling of blood plasma is also possible via injections of high molecular weight fluorophores in the vascular circuit (fluorescent nanoparticles, conjugated DEXTRAN, etc.). A final example of *in vivo* labeling may be the injection of tetracycline which tends to fix itself to the bone portions which are freshly renewed. However, the list does not stop there and new fluorescent probes regularly appear in the catalogs of different manufacturers.

1.3.3. *Practical implementation of confocal microscopy*

1.3.3.1. *Introduction*

Above all, it must be said that it is difficult to quantify simply the capacity or limits of a confocal microscopy system. Since their introduction in the 1980s, these systems have evolved with advances in automation and information technology, of course, but considerable effort has also been expended to maximize the fluorescence photons collected [PAD 08]. Consequently, current systems have very good general characteristics. Their resolution is essentially limited by diffraction, lasers are rarely used at full power to avoid damaging the samples or the fluorophores, a large majority of the fluorescence photons is collected by high numerical aperture

objectives, the other elements of the chain of detection also have good optical transmission and, finally, the detectors can almost count photons. Although there are still optimization efforts to make here and there, we can say that these systems are not limited by the laser power available or by the sensitivity of the detectors. To a lesser extent, it becomes very difficult to improve further the transmission of the chain of detection or the resolution of objectives (already capable of collecting the light in an almost half-space!). Under these conditions, the limits of this method are not really technological limitations.

Yet, it is true that each manufacturer has chosen different strategies and comparisons can be made between existing systems. Some have chosen sensitivity while others rely on speed, ergonomy or price. Despite this, and imagining an "ideal" confocal microscope combining the best of all systems, the issue of instrumental limitations for a system of confocal laser scanning microscopy is not a very relevant issue in the context of this book. In addition, the notion of an "ideal confocal microscope" depends upon the application. With the variety of biological topics, samples of tissues or cells and, finally, fluorescent probes and labeling techniques, a more interesting question is to ask ourselves what are the possibilities and limitations of confocal laser scanning microscopy for a given application, a given sample and a given label. However, it would be too long and complex and certainly unsuccessful to attempt to review every application of confocal microscopy in biology! Only bibliographic research, testing and experience can truly identify the potential and limitations of confocal laser scanning microscopy in a given framework.

However, it is of course possible to discuss the capabilities and limitations of confocal microscopy in addressing a number of key issues common to most applications. To do this, we have chosen to illustrate our discussion with different observations of the same test sample. This sample is a section of 30 micron-thick fixed plant tissues labeled by two fluorescent stable molecules. This tissue is placed between a slide and a coverslip. All images in this section were obtained using a × 63 oil immersion objective with a numerical aperture of 1.40 to obtain the best possible resolution. Whilst the following section has no biological interest, the purpose of this "case study" is purely educational and a pretext to addressing the practical implementation, interests and limitations of the method. This approach aims as a guiding principle to compare different modes of imaging, illustrate

certain limitations specifically and describe approaches for evaluating the performance of the system. However, each characteristic, limitation or type of adjustment will be addressed in a broader discussion allowing us to talk about problems that might be encountered and the solutions that exist in other situations.

1.3.3.2. *Comparison of contrast modes*

Figure 1.4 shows a comparison between the methods of wide-field microscopy (bright-field (Figure 1.4a) and epifluorescence (Figure 1.4b)) and the modes of confocal laser scanning microscopy (Figures 1.4c, 1.4d, 1.4e and 1.4f). The most striking element when we compare these microscopy modes clearly concerns the contrast, i.e. the ratio of luminosity between the lightest and darkest areas. Wide-field images appear less contrasted and include less detail, because they are blurred by refraction effects through the turbid medium (in the case of bright-field) and by halos of light coming from fluorescence outside the focal plane (in the case of epifluorescence). In epifluorescence, we observe certain structures which are highly fluorescent in the confocal images (small grains of a few microns in diameter) with great difficulty. Thus, it is important to note that confocal microscopy effectively provides a contrast enhancement by eliminating stray light coming from planes far from the object plane of the microscope. However, the improvement goes far beyond a simple contrast gain since in some samples (like this one) unwanted light makes it very difficult to spot smaller objects which provide very little fluorescence. The improved resolution (see the previous section on resolution) is only secondary and when observing objects of the order of a micron (bacteria, for example) scattered in a single layer on a slide, the contribution of confocal microscopy is not always obvious. However, when it comes to tissue slices whose thickness is more than a couple of micrometers, the potential of optical sectioning becomes interesting, not necessarily because the resolution limit is slightly better, but because the contrast is improved, better controlled, and especially because small structures usually embedded in the fluorescence of the whole sample can be revealed.

Confocal microscopy provides another interesting mode of contrast that is sometimes overlooked. It is simply the reflection or backscattering contrast. The laser scans the sample and the light is collected at the same wavelength (using a semi-reflecting plate and not a dichroic mirror). In our sample, this method of contrast is illustrated in Figure 1.4c, which represents an average

projection of 40 stacked images obtained within a total thickness of 15 microns. This contrast mode therefore gives a very different image from fluorescence images and, most importantly, does not require labeling. In the case of our image, for example, certain parts, which seem to be plasma membranes, are visible while the thick supporting walls, characteristic of plant tissues, return almost no signal, because they are highly transparent and positioned perpendicularly to the beam. It is necessary to remain cautious about the interpretation of an image obtained by reflection because it is a complex mixture of information obtained by reflection and backscattering from the different inhomogeneities of tissues at the submicron scale [DUN 96]. However, the imaging principle is sometimes useful in addition to fluorescent tagging to localize unlabeled structures or the sample surface and to characterize the roughness of this surface. Some interesting works have focused on this mode to characterize variations of diffusion properties in tissue [COL 05]. These variations in the optical properties of tissue may come from a change in size and/or shape of the cells and modifications in intracellular complexity. This kind of approach is very interesting for the characterization and identification of cancerous tissue, for example.

1.3.3.3. *Experimental resolution*

Figure 1.4f reveals clearly the contribution of contrast confocal microscopy, especially by the revelation of very fine structures (most likely cell membranes, hence with a thickness of about 10 nm). These structures allow us to evaluate the experimental resolution of the instrument by performing the spatial profile of a fine structure of the image in Figure 1.4f. This spatial pattern is shown in Figure 1.4h. Presumably it represents the point spread function (or PSF) of the instrument and measures approximately 190 nm at half-maximum. The width of the experimental PSF can be compared with the theoretical resolution of the order of 140 nm in this case. Thus, there is a good agreement between theory and experiment.

However, we always measure a resolution slightly higher experimentally [KOZ 01]. With objectives of high quality and high numerical aperture, it is in fact very difficult to maintain the right conditions for focusing a laser beam without aberrations. A coverslip of thickness higher or lower by only 10 microns compared with what the manufacturer recommends, a mounting medium with an inadequate index, a poorly chosen immersion medium and spherical aberrations can appear and can quickly modify the resolution. The observation depth also affects the resolution and therefore it is impossible,

strictly speaking, to maintain a fixed resolution when making a stack of images of 100 microns thickness. The homogeneity of the incident laser beam and how it is truncated by the microscope objective are other possible causes of a modification to the experimental resolution compared with the theoretical resolution. Finally, when we attempt to measure the experimental resolution, it is not always easy to find objects both fluorescent enough and small enough to measure a true impulse response function [KOZ 01]. However, it may be important to do this when you want to apply to images certain digital deconvolution algorithms.

Finally, it should be noted that the notion of experimental resolution is closely linked to the concept of signal-to-noise ratio in images and therefore to the notion of contrast [STE 98]. Indeed, how can we set a value representing the experimental resolution when using a low dynamic and very noisy signal? In summary, the laws of diffraction allow us to determine the theoretical maximum resolution that we can hope to achieve with a given system and with ideal observation conditions. If these conditions are not ideal, an experimental resolution can still be defined and characterized, but in extreme cases where the contrast is degraded, it may be impossible to characterize the experimental resolution properly.

1.3.3.4. *Scanning, zooming and image format*

To plot the spatial profile of Figure 1.4h, it was necessary to use a sampling above the resolution limit of the instrument. This was made possible by zooming in on a particular area of the sample. Even if the time of acquisition is limited by the scanning speed, it gives scanning microscopy a great flexibility in sampling images. Indeed, the scan is configurable in terms of speed and in terms of the size of the area scanned. In addition, the analog signal recorded during scanning of a line can be sampled in a range going typically from 16 to 4,096 points (powers of 2)[3]. The objective used here allows a resolution of the order of 190 nm and a field of view of 240 microns. The famous Nyquist-Shannon sampling theorem indicates that it is necessary to take at least two points per 190 nm scanned to have a sampling adapted to this optical resolution of 190 nm. Here, it is therefore necessary to make a sample of 2,526 points per line to be at the limit of resolution whilst observing the full field offered by this objective. If the application requires

3 These are the format sizes required by our system, but any other sampling could be considered within the limits of capacity of the system of acquisition.

taking full advantage of the system resolution, then there are two possibilities: either to choose an image format with sufficient pixels and enjoy the whole width of the field, or select a sampling with fewer points, but also reduce the scanned field, i.e. perform a zoom. In the case of the image in Figure 1.4f, a zoom factor of 4 and an image size of 1,024x1,024 were selected, i.e. an image of 1,024x1,024 pixels has been formed on a field of 60 microns and no longer on 240 microns. In this case, the final image has one pixel every 60 nm, in order to meet the Nyquist-Shannon criterion.

However, adjusting the parameters of scanning and sampling must not be solely guided by considerations of adaptation between resolution and sampling. Indeed, when selecting a greater zoom factor, a smaller area is scanned, but with the same horizontal scan rate (expressed in Hz or lines per second). Under these conditions, the laser beam stays longer on each point of the image, which allows us to collect more fluorescence by point, but can also precipitate possible photodamage. However, scanning with a smaller field can also, technically, increase the scanning speed of the scanner (because you can make it vibrate faster without exceeding its mechanical limits). Consequently, it is possible, when we increase the zoom factor, to also increase in parallel the scanning speed to the maximum it can achieve. This allows us to scan faster whilst keeping a similar dwelling time on each pixel. However, if it is the luminosity that is sought rather than speed, it is better to maximize the dwelling time, but always within the limits of resistance to photodamage of the fluorescence probe.

Finally, it should also be noted that in choosing a sampling with fewer points, we lose in resolution, for sure, but we gain in brightness, as the gray level of each pixel is coming from fewer points on the same analog signal. Accordingly, the settings of the zoom factor, the scanning speed and the image size must be adjusted according to the constraints of the biological study to be carried out so as to achieve a compromise in order that resolution, field scanning, speed acquisition and brightness are sufficient without inducing photodamage to the sample. In many applications, we do not ask ourselves all these questions when the image is correct, but if you want to push confocal microscopy to its limits, we cannot do without these considerations.

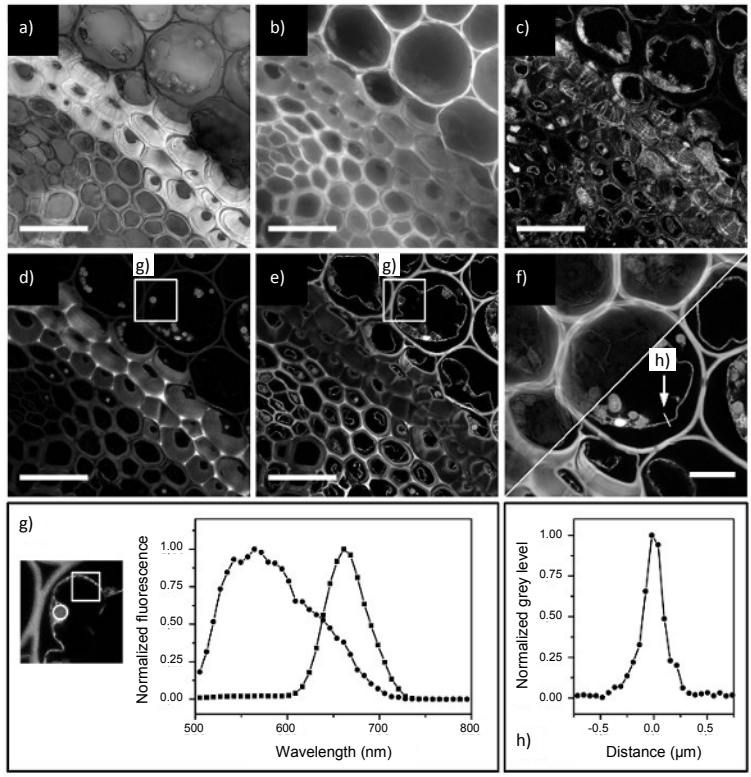

Figure 1.4. *Various observations of the same plant sample with two fluorescent labels: a) bright-field; b) epifluorescence; c) confocal microscopy (reflection); d) confocal microscopy (fluorescence in the green-yellow band); e) confocal microscopy (fluorescence in the orange-red band); f) comparison between epifluorescence/confocal on a zoom (scale bar is 10 microns); g) fluorescence spectra obtained on the areas indicated by the circle and the square; h) spatial profile obtained along the segment shown in image f). Unless otherwise specified, scale bars are 30 microns*

1.3.3.5. *Spectral separation*

The problem of spectral separation between excitation light and fluorescence, and then between different bands of fluorescence with different labels, is essential in this kind of method. Indeed, it is a major source of artifacts and misinterpretations of images, since a poor removal of the excitation light or a spectral superposition of two fluorescence spectra can give the impression that some areas of the image have been labeled by a given fluorophore when they are not, or in any case not by the fluorophore expected. This problem of spectral separation can be addressed by going

back to Figures 1.4d and 1.4e. The two images shown were obtained using the fluorescence in a band ranging from 500 to 590 nm for Figure 1.4d and from 600 to 750 nm for Figure 1.4e. We can clearly distinguish that these two images provide contrast in quite distinct areas. This is a reflection of the double labeling which was performed on this sample and which seems to divide it into two bands of fluorescence, one rather yellow-green and another one in orange-red. The confocal system which has been used here allows precise control of the spectral bands of fluorescence impinging each photodetector. The flexibility of the system of spectral separation has also allowed us to achieve a series of images by reducing to 10 nm the spectral window for collection and by shifting it from 500 nm to 800 nm. It is therefore possible to plot the fluorescence spectrum of the sample for two areas, each providing fluorescence spectra in a specific band (see the circular and square areas in Figure 1.4g). The appearance of the spectra indicates immediately that the excitation light at 488 nm has been properly removed. This is not always the case and when the fluorescence of the fluorophores is too low, it is not uncommon for the wings of the excitation laser line to appear, even if the wavelength scan starts 10 nm after the central wavelength of the laser line. In such a sensitive system, even a tiny fraction of the excitation light can become significant compared with the quite low fluorescence. This is why it is essential to use dichroic mirrors with a high rejection rate. *Acousto-optic beam splitter* (AOBS) systems present a significant opportunity to push yet further the separation between excitation light and fluorescence.

Even once the excitation light has been properly eliminated, it remains to ensure that the fluorescence bands of different fluorophores are separated. Figure 1.4g shows, however, that the first fluorophore exhibits fluorescence up to 700 nm. If the first measurement channel involves only the fluorescence of the first fluorophore between 500 and 590 nm, the second channel, involving fluorescence between 600 to 750 nm, includes a mixture of the two labels. This is effectively observed on the images of Figures 1.4d and 1.4e; areas appearing in Figure 1.4d are also visible in Figure 1.4e. This phenomenon of fluorescence spectral overlap is quite common and can become very annoying when, for example, we seek to study co-localization, i.e. we attempt to identify with the greatest possible certainty the areas where the two tags appear together. In addition, if the first green-yellow label was much brighter than the other, the problem could become catastrophic as the orange-red fluorescence would be completely embedded in the neighboring fluorescence. To limit this kind of artifact arising from the overlap of the

labels, it is possible to use fluorophores whose fluorescence spectra are quite distinct. However, this is not always possible, especially if the sample must contain three or four tags. In the latter case, the use of nanoparticle labeling (quantum dots) can limit the spectral overlap because they have narrower luminescence spectra. Another approach is to make sequential acquisitions of images with different excitations: an image of the first fluorescence is recorded normally, then in a second step, a second image is recorded with a higher excitation wavelength, more adapted to the excitation of the second fluorescent tag, and especially, not exciting at all the first fluorescent tag. In our case, the phenomenon of overlap would certainly have been limited by using an excitation at 543 nm to reduce the fluorescence of the first fluorophore. Finally, there is also a software solution to reduce the effects of spectral overlaps. Indeed, the production of a series of images according to the wavelength used allows us to determine the fluorescence spectrum for each pixel. *A priori* knowledge of the fluorescence spectra of different fluorophores allows us then to perform a digital spectral separation of the different fluorescence tags. As with any numerical method, this kind of algorithm will work better or worse depending upon the importance of the artifact, the quality of the images and the *a priori* knowledge of the fluorescence spectra.

1.3.3.6. *Detection, signal to noise ratio and imaging depth limit*

In a system of confocal microscopy, collected fluorescence at a given point comes from a focal volume of the order of a femtoliter (see sections dealing with the resolution) and in this volume, only a small handful of sites may have been labeled, which may represent just a few million to a few fluorescent molecules at a given point. The fluorescence collection is done, at best, through a half-space and through a large amount of optics, a dichroic mirror and a dispersive element. Under these conditions, the fraction of fluorescence that reaches the detector is often quite low. However, scanning one point at a time allows us to use photomultipliers or avalanche photodiodes that offer high sensitivity, since they are capable of detecting almost one photon (although most commercial systems cannot work in a real controlled photon counting mode).

With good labeling and good scanning parameters (especially in terms of dwelling time on a pixel), fluorescence flow is often sufficient to use photomultipliers with a relatively low gain. In this case, the background noise, which may come from stray light or from thermal noise of the detectors, may remain well below the fluorescence signal. It is difficult to

give a maximum signal-to-noise ratio in confocal microscopy because this parameter is highly dependent on the types of detectors, technological solutions selected by the various manufacturers and the mode of use. However, most systems of confocal microscopy offer the opportunity to sample the signal on at least 12 bits (4,096 gray levels) instead of 8 bits (256 gray levels) for classical imaging systems. Indeed, manufacturers estimate that under ideal conditions of use, a lower number of gray levels could produce a limitation on the system dynamic. To say that the maximum signal-to-noise ratio is typically at least 4,096 is a bit premature. Furthermore, is it actually relevant information? When it comes to simply localizing the labeled areas, and caricaturing a little, working on thresholded binary images may suffice. Under these conditions, a signal-to-noise ratio greater than two is sufficient. By moving to a more realistic argument, it is more convenient or even necessary to work with a signal-to-noise ratio greater than two, especially if the images must undergo digital processing (spatial deconvolution, for example), if the fluorescence spectra is sought or in the case of certain applications that require quantitative evaluation of the fluorescence (using ratiometric probes, for example).

In such cases, the question of signal-to-noise ratio is actually more relevant. This determination is still difficult to assess theoretically and depends upon several parameters of the detection system, experimental conditions, sample and imaging depth. The purpose here is not to lecture on the different sources of noise in an optical system whose detection is carried out by photomultipliers or avalanche photodiodes. However, it is possible to quickly review the main sources of noise which will significantly influence the signal-to-noise ratio in confocal microscopy. For a significant collected throughput of light, the gain of the photodetectors can be set relatively low and, in this case, the dark noise (superposition of thermal noise, electronic noise and stray light entering the system) remains very moderate, even negligible. Some manufacturers even offer detectors with a low-temperature cooling system, which can greatly reduce this source of noise. Signal noise, in turn, is mainly owing to fluctuations of the lasers, which can also be very moderate and do not really constitute a limiting factor for most common uses.

In confocal microscopy, working with low luminosities is very common and it is in this case that the noise will actually become a problem. Indeed, at low light and with high gain photodetectors, the dark noise will reach its maximum level. The sensitivity of photodetectors requires working in

complete darkness and, despite this, the thermal noise becomes visible. It can however be quickly eliminated by a few averages of lines or images. The different noise sources mentioned above are not the most troublesome and will be highly dependent on equipment (photomultiplier detector or avalanche photodiodes, cooled or not, electronics and quality of components, the presence of stray light, etc.). In low light conditions and in all systems, it is the shot noise (or quantum noise) which becomes dominant and primarily responsible for limiting the signal-to-noise ratio. Indeed, it is not uncommon to collect only a few photons during the dwelling time on a pixel. In such cases, the signal collected during the dwelling time of the beam on a pixel follows a Poisson distribution.

This problem is illustrated in Figure 1.5. We still choose to work with the same sample with a quick scan and a very low excitation power to push the photomultipliers to their maximum gain. Figure 1.5a is a raw image obtained under these conditions. The main structures are still visible, but the images have an almost binary distribution of their gray levels. With such a low photon flux and such sensitivity, the gray levels of pixels are divided into two main categories: pixels which are almost white (detection of a photon) and pixels which are almost black (no photon detection). The images have been thresholded and averaged over two, five, ten, fifty and a hundred images (Figures 1.5b, 1.5c, 1.5d, 1.5e and 1.5f). Thanks to accumulations, the image was of an acceptable quality (Figure 1.5f). However, a deliberately pixelated magnification (Figure 1.5g) of the accumulation of a hundred images indicates that the standard deviation of the gray levels is important. Indeed, in the case of a Poisson noise, the statistic distribution increasingly approaches a Gaussian distribution as we accumulate images. Unfortunately, the Poisson distribution imposes a variance equal to the average. This is illustrated in Figure 1.5h which shows the statistical distribution of the number of hits (lit pixel) that have been accumulated on each pixel in the specified areas of interest in Figures 1.5d, 1.5e and 1.5f. The solid lines represent a fit with the Poisson law indicating that on average, during the acquisition of an image, approximately $\lambda = 0.18$ hits were counted in this area per pixel. If the signal-to-noise ratio is defined as the ratio between the average and standard deviation, it is limited to a value of the order of $\sqrt{N\lambda}$, where N is the number of accumulated frames. In our case, the accumulation of one hundred images provides a signal-to-noise ratio of about 4.3. At a rate of one image per second, a quick calculation tells us that we will require more than 15 hours of accumulation

to find a signal-to-noise ratio of the order of a hundred! Under these conditions, any quantitative use requiring the monitoring of fluorescence pixel per pixel becomes difficult. Similarly, the difficulty of obtaining a good signal-to-noise ratio can become very problematic when the images are intended to undergo treatment or subsequent computer analysis (thresholding, segmentation, automatic counting of particles, deconvolution, etc.). However, in considering the average levels of signal in larger areas of interest, with many pixels, all quantitative work in low light remains possible. It is then up to the user to optimize each experimental parameter, and the size of the areas of interest to study.

From the concept of signal-to-noise ratio derives naturally the notion of the imaging depth limit in confocal microscopy. Indeed, even if the signal-to-noise ratio is large enough on the surface of a sample, there always comes a moment when it becomes critical when attempting to observe deeper areas in a thick scattering tissue. This arises from the fact that as soon as we seek to image the depth of a tissue, the losses by absorption and light scattering quickly reduce the level of collected fluorescence. Meanwhile, the filtering pinhole which eliminates the fluorescence out of the object plane increasingly struggles to function, because the fluorescence on the surface rapidly becomes more important than the fluorescence from the object plane. A background noise therefore gradually appears whilst the fluorescence signal decreases. This loss of signal-to-noise ratio will determine the imaging depth limit of confocal microscopy. The imaging depth limit can then be defined as the depth at which the signal-to-noise ratio becomes equal to one. Thus, the maximum depth is, to a large extent, dependent upon the scattering and absorption properties of the sample. In most biological samples, it is the scattering which is the main source of loss of light in the focal volume [CHE 90]. The scattering properties of biological tissue can be quantified by the reduced scattering coefficient whose inverse is the mean free path of a photon between two events of isotropic scattering [PAT 89]. Depending upon the type of biological tissue, the reduced scattering coefficient can vary typically from $1cm^{-1}$ to $60cm^{-1}$ [CHE 90], which corresponds to a mean free path of the order of 170 microns to 1 cm. We also know that the amount of non-scattered photons follows a law of exponential decay as $\exp(-z/l_s)$, where z is the height from the surface of the scattering sample and l_s is the mean free path. It is therefore reasonable to assume that the imaging conditions are severely degraded when the imaging depth exceeds two or three times the scattering mean free path [SMI 98]. Combining all this information, a penetration limit of the order of several

hundreds of microns to several centimeters appears to emerge, but this is a very theoretical value, assuming ideal imaging conditions, very efficient labelings and perfectly flat samples whose distribution remains uniform over a thickness of hundreds of microns. In addition, these theoretical limits cannot always be reached in many common situations. For example, immunocytochemical labelings are made through large molecules (antibodies) that do not penetrate more than a few cellular layers (approximately 50 microns).

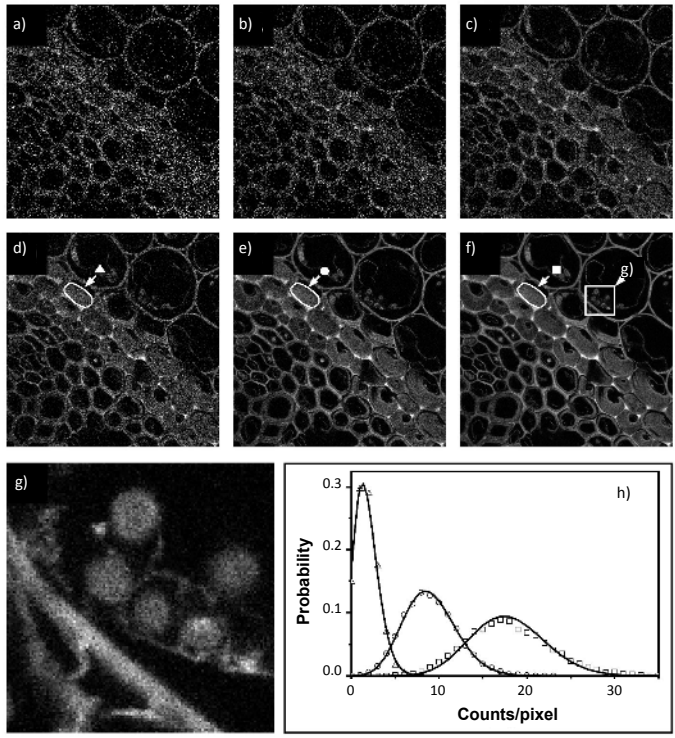

Figure 1.5. *Confocal images obtained with a low level of fluorescence and a photomultiplier gain pushed to maximum: raw image (a), average of two images (b), five images (c), ten images (d), fifty images (e), and a hundred images (f). Figure g) shows an enlargement of the area shown in figure f) and figure h) represents the statistical distribution of gray levels in the areas shown in images d), e) and f) (dots: experimental data, solid line: theoretical model with a Poisson distribution)*

Another example of a technical limitation, a microscope objective of high numerical aperture allows a good collection of fluorescence, but rarely has a working distance greater than 200 microns (except for those special

objectives with high numerical aperture and long working distance). Generally, it can be said that it is difficult to achieve imaging depths that exceed 50 microns [DAI 06], although some studies present quite noisy images at depths of about 100 microns [COL 05]. Finally, if you are looking for a very good resolution and/or high contrast, the notion of imaging depth limit defined above by the total loss of contrast must be replaced by another, more restrictive, limit.

1.3.3.7. *Tomographic aspects*

This section on the practical implementation of confocal microscopy cannot be completed without a few remarks on tomographic and three-dimensional aspects. The ability to make virtual slices with thicknesses of the order of a micron makes confocal microscopy a tomographic imaging method, and through the creation of stacks of serial images, volume reconstructions are possible. This feature is often at the origin of the popularity of this method. However, despite the beautiful three-dimensional animations that result, we must not lose sight of the true scientific interests of the tomographic aspect or of some related difficulties and artifacts.

Figure 1.6 illustrates the tomographic aspects of confocal microscopy. Figure 1.6a shows a series of images taken with an increment of the order of 1 micron and still on our sample of plant tissue. In this series, it is clear that the brightness of the image decreases with depth, as no compensation for losses by absorption and scattering has been performed. However, it is possible to compensate for this loss, to some extent, by incrementing the laser power and/or the photomultiplier gain as we gradually penetrate the sample. This loss of brightness is also clearly visible on the projections in Figure 1.6b, which represents a first possibility of three-dimensional exploration of our series of images. This figure shows an optical slice and perpendicular sections in the YZ and XZ planes obtained along the lines drawn in white. Thanks to the XZ section, in particular, it was possible to verify that the loss of brightness follows roughly a decreasing exponential, which is typical of losses by absorption and light scattering. Thanks to these sections, we further note that the brightness is divided by ten after about 30 microns of penetration in the dense parts of intercellular areas. This gives a rough order of magnitude of the imaging depth limit in this sample.

This type of perpendicular projection enables us to highlight a typical artifact in confocal microscopy: the difference between the axial resolution

and lateral resolution (see the section on resolution). However, in Figure 1.6b, this problem is not really visible because the smaller objects are spheres of 5 or 6 microns in diameter, or about ten times the theoretical axial resolution. When one creates, however, images of objects of similar size or smaller than the lateral resolution, the XZ and YZ sections may look blurred in the direction of the Z axis. This is because the axial resolution is always greater than the lateral resolution. The ratio between axial and lateral resolution depends upon the numerical aperture of the objectives. It typically varies between 3 and 5 in the best cases, but can quickly exceed 10 or 15 when the numerical aperture is less than 0.5. In this case, a spherical object smaller than the resolution will appear on a XZ section as an ellipse 10 to 15 times taller than wide! When the application requires it and the images are suitable, the three-dimensional spatial deconvolution can reduce this problem.

Figures 1.6c, 1.6d and 1.6e show three types of commonly used projection for stacks of confocal microscopy images. Figure 1.6c is simply an average projection, i.e. the average of all images in the series shown in Figure 1.6a. Depending upon needs, this mode of projection can also be done in several different ways, using for example the median or the maximum rather than the average. This is the most obvious projection mode and it is very commonly used. The tomographic information is lost, but an image is obtained integrating information on the whole image stack. It then offers a full view of the sample in which all planes are focused, which overcomes the lack of depth of field of wide-field microscopy. To find tomographic information with this type of axial projection, it is possible to use algorithms that associate various colors with the depth. There are also methods of projection which axially localize the position of maximum brightness or even the center of gravity of the brightness. This gives a true tomographic image which associates a gray level with an axial position, which is particularly suitable for studies of interfaces or surface roughness.

The projections in Figures 1.6d and 1.6e are, in turn, axonometric perspectives of the stack of images (regarded as a volume) observed with a small angle of rotation around the Y axis. The projection in Figure 1.6d is a transparent projection, i.e. we associate with each voxel (volumetric equivalent of a pixel) a level of transparency even more elevated when its gray level tends towards 0. Figure 1.6e is an opaque projection that uses thresholding, a bright texture mapping and artificial lighting effect. Accordingly, this type of projection represents a three-dimensional view of

the surfaces of the fluorescent objects. It should be noted that this type of opaque projection will not show the difference between a full or hollow sphere, for example, unless a well-chosen volumetric sector is removed from the picture, or made partially transparent. Depending upon the samples, applications and tools at his/her disposal, the user must choose the type of pre-treatment to perform on his/her stack of images (deconvolution, volumetric smoothing, thresholding, etc.), and the type of three-dimensional projection, viewing angle and slices which will allow him/her to reveal the most relevant scientific information contained in the image stack.

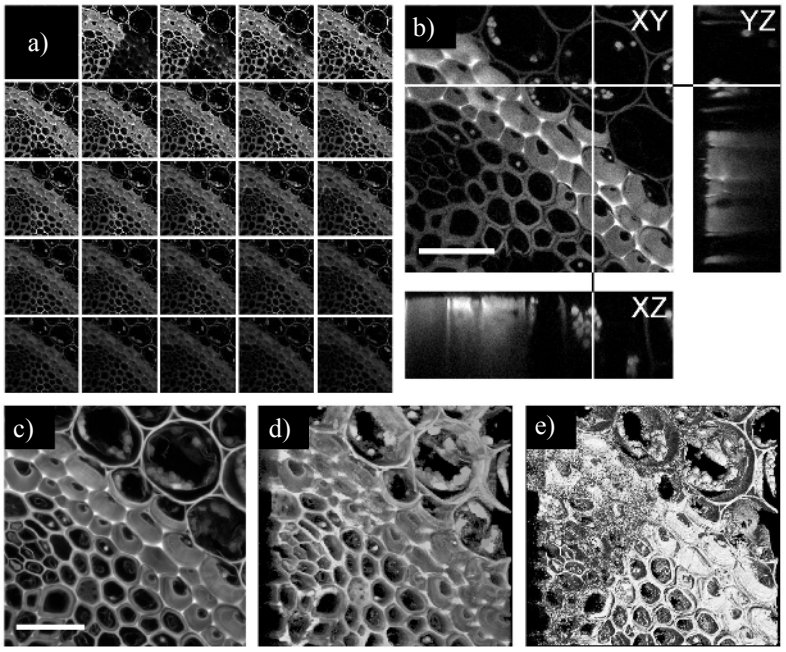

Figure 1.6. *Projection and three-dimensional aspects of our plant sample (scale bar: 30 microns): a) raw stack of confocal images depending upon the depth (increment ≈ 1 micron); b) observation of the stack in the form of sections (XY , YZ and XZ); c) average projection (average over all the images in the stack); d) three-dimensional projection with volume rendering in transparent mode and viewed with a slight angle of rotation along the vertical axis; e) other type of three-dimensional projection with volume rendering in opaque mode (thresholding, texture mapping and effect of artificial lighting)*

To conclude on tomographic aspects, it is necessary to say a few words about the acquisition time and the volume of data generated in confocal

microscopy. Indeed, we have seen that the imaging speed is quite limited, either by technological aspects (scanning capacity of the galvanometer mirrors) or by too weak a fluorescence, which then requires staying longer on a single point to collect enough photons. Under these conditions, the production of stacks of several hundred images can quickly become very long, especially if each image of the stack itself results from an average of several images. Consequently, with a typical acquisition rate of about one frame per second, averages of 20 images and a stack of 200 sections, we arrive at a total acquisition time of about an hour. If we add to that a sequential acquisition with several different and alternate excitations (to minimize, for example, spectral overlaps), we reach an acquisition time multiplied by the number of acquisition sequences. In addition, the amount of computer data then reaches 400 MB, just for a single stack (8 bits, two channels and a sampling of 1,024x1,024 pixels). Without becoming prohibitive in most cases, these temporal and computing aspects can become critical, especially if the experiments carried out require, in addition, recording stacks as a function of time (to study modifications in live samples, for example), as a function of the transversal position of the sample (to record z stacks mosaic and therefore broaden the field observed), or even as a function of the wavelength of emission (if the experiment requires detailed analysis of the spectra of collected fluorescence). To minimize acquisition time and the amount of data, it will be necessary to make a careful choice of parameters for scanning, sampling and storage, which will require more than ever having a thorough knowledge of the method of confocal microscopy and its limits.

1.4. Related and derived techniques

1.4.1. *Advanced contrast modes: FRAP, FLIP, FLIM, FRET, etc.*

We have seen that confocal laser scanning fluorescence microscopy can offer a reliable and well controlled contrast and a possibility of axial resolution that epifluorescence microscopy does not allow. In addition, the use of laser scanning allows a flexible and precise control of the light deposited on a sample. Finally, the luminescence being recorded one point after the other, we can imagine analyzing other information conveyed by this light: its spectrum, its decay time, its anisotropy, its polarization, etc. (all information that would be impossible or complicated to analyze by classical wide-field detection). Thus, control of the incident beam and the flexibility

of single-point detection paved the way for the development of other types of contrast based upon a more detailed analysis of fluorescence characteristics or on the use of fluorophores with unique properties. Without going into too much detail and variations of these different modes of contrasts, we will describe the general principle of some of these techniques. For more information, the reader is referred to more detailed articles [TRU 04].

The Fluorescence Recovery After Photobleaching (FRAP) and Fluorescence Loss In Photobleaching (FLIP) techniques are both based upon a voluntary and localized extinction of fluorescence, i.e. a photobleaching in a chosen area of a fluorescent sample. This is made possible by a repeated and more powerful laser scan in an area of interest previously selected by the user.

In the case of the FRAP technique, a lower laser power is then restored. First, a dark area is observed where the extinction was induced. Then this dark area can gradually regain a level of fluorescence lower than or equal to its original level because it is, little by little, repopulated by diffusion, by fluorescent molecules nearby. By analyzing the repopulation time and comparing the levels of fluorescence before extinction and after repopulation, it is then possible to deduce information on the mobility of labeled molecules and on the fractions of mobile and immobile molecules.

In the case of the FLIP technique, this is the loss of fluorescence which is studied while photobleaching occurs. Depending upon the circumstances, these measures may help to deduce information on the interactions between the labeled molecule and its environment (size of the labeled molecule, links to other molecules, cellular compartments, localization of a cellular compartment by variation in viscosity, interactions between two compartments, etc.). These techniques can provide a more quantitative dimension to confocal microscopy which, more than ever, allows us to deduce more functional information than structural information.

Finally, it should be noted that these techniques do not require any special adaptation: any confocal scanning microscope allows such studies, once the scanning is fast enough and the incident laser power is controlled by software. However, it is necessary to choose the fluorophores well so that they do not photobleach either too quickly, or too slowly, adjusting the power, number and rate of scans necessary to quench the fluorescence. Then,

it is necessary to be able to follow the dynamics of repopulation or the loss of fluorescence with sufficient temporal resolution. Like any method based upon a quantitative evaluation of the fluorescence, it is also necessary to optimize the acquisition parameters and to use fluorophores with good absorption and good fluorescence efficiency (see the section on signal-to-noise ratio in confocal microscopy).

The Fluorescence Resonance Energy Transfer or Förster Resonance Energy Transfer (FRET) technique consists of using a couple of fluorophores, one of which (called the donor) is able to transfer part of its energy to a second (called the acceptor). This phenomenon is at a maximum when three conditions are met: the emission band of the donor must partly overlap the absorption band of the acceptor, the two molecules must be separated by less than 2 to 6 nm (typically) [HIB 04] and finally, a particular condition of orientation for the two molecules must be fulfilled. Thus, if these two fluorophores have been linked to other molecules of interest (for example, two proteins), an interaction between these two molecules may result in a decrease in the emission of the donor in favor of the acceptor. As the two fluorophores do not have the same emission band, it is sufficient to study the fluorescence ratio in two measurement channels (one for the donor fluorescence and the other for the acceptor fluorescence). Just as for the FRAP and FLIP techniques, this method does not require special adaptation of the optical system of the confocal microscope. However, it will give more robust results if it is combined with the FLIM technique described in the next paragraph. In addition, there are approaches to confirm FRET effects when the measurements of fluorescence ratios remain ambiguous. These approaches consist of inducing photobleaching of the donor or the acceptor. In the case of a donor photobleaching, the proximity of the acceptor induces donor resistance to photobleaching. The decay of donor fluorescence is then lengthened in the presence of the acceptor. In the case of photobleaching of the acceptor, the donor will emit more fluorescence as the extinction of the acceptor with which it interacts progresses.

The Fluorescence Lifetime Imaging Microscopy (FLIM) technique is another derived technique based this time not on the measurement of the intensity of fluorescence, but on its decay time. For most fluorescent molecules, this time is typically of the order of nanoseconds and is specific for a given molecule (more particularly of the characteristics of the quantum state brought into play in the process of fluorescence). However, when the molecule is not isolated (as is always the case in practice), the interaction of

this molecule with its environment leads to modifications in the fluorescence characteristics and particularly to changes in the fluorescence decay time. Indeed, energy transfers are possible to other molecules, offering non-radiative relaxation modes that deplete the fluorescence of the considered molecule faster. Thus, changes in the fluorescence decay time of a given molecule will be related to the interactions with other molecules in its environment. Besides the ability to deduce information on the interactions of a molecule of interest with another molecule of the environment or other intracellular structure, this mode of contrast provides a signal that is more objectively linked to a given molecule in a given molecular context and more robust towards artefactual variations of the level of fluorescence. Notably, this contrast mode is often associated with the FRET technique described above [BOR 02]. Indeed, the interaction between a donor and an acceptor is also detectable by a decrease in the decay time of the donor, for example, which reflects the energy transfer to the acceptor.

The implementation of such a technique requires modifications to the basic configuration of confocal microscopy because it is necessary to modulate the excitation and implement a fluorescence detection which is resolved in time and with a resolution of the order of tens of picoseconds. To do this, there are two approaches, one in the time domain and another in the frequency domain. In the case of measurement in the time domain, the excitation of the fluorophores is caused by laser pulses of a picosecond or even femtosecond duration. Measuring the decay time then requires a detection device that allows us to resolve the decay, thus a temporal resolution of the order of ten picoseconds. The excitation can be done through pulsed laser diodes, oscillators with solid-state gain media (typically titanium doped sapphire) or pulsed fiber lasers in the near infrared, but coupled to modules which generate white light supercontinuum. Regarding detection, the most common method used is based upon the implementation of a time-correlated single-photon counting setup, whose principle is to measure the average time between the incident pulse and a re-emitted fluorescence photon [BOR 02]. The other approach, in the frequency domain, consists of modulating a continuous incident beam (either directly in the case of using laser diodes, or by means of an acousto-optic modulator, for example) and measuring the phase shift between the incident modulation and the modulation of light remitted by fluorescence using a lock-in amplifier.

1.4.2. *The contribution of nonlinear contrast modes*

Since the 1990s and the article by Denk [DEN 90], a new method of contrast has appeared, which has been considerably developed and expanded [HEL 05 ZIP 03]. This contrast is based upon the excitation of nonlinear optical properties, such as two-photon absorption. In this absorption mechanism, predicted since the 1930s by Maria Goeppert-Mayer [GOP 31], two photons can interact and combine their energies within a molecule to reach excitation states normally achieved with photons twice as energetic. Consequently, a photon of a blue radiation at 450 nm, for example, carries the same energy as two combined photons coming from a light in the near infrared at double the wavelength, namely 900 nm. However, the probability of having two photons arriving at the same time and on the same molecule is particularly low with a continuous light source, which makes this mechanism very marginal and even impossible to observe with such a light source. It is therefore necessary to use a focused pulse laser which can concentrate in time and in space the photons and make this absorption mechanism not negligible. One of the first noticeable effects on laser scanning fluorescence microscopy is that two-photon absorption is negligible in areas where the beam is wider transversely. The mechanism of two-photon absorption is then only significant in the area where laser power is most concentrated, i.e. around the focal point. Only fluorescent molecules localized inside the focal volume are capable of absorbing light by a mechanism of two-photon absorption and the re-emitted fluorescence results essentially from the fluorescent molecules localized in the focal volume. This particular property (which comes directly from the fact that two-photon absorption is a nonlinear phenomenon) implies that contrasts based upon nonlinear effects come essentially from the imaging plane alone. Unlike the case of confocal microscopy with linear contrast, it is no longer necessary here to filter the light coming from out of focus planes with a confocal pinhole. This light can therefore be directly collected just after its return to the objective (or directly in transmission behind the sample when it is possible), without having to go through the scanner, the filtering pinhole and all the other elements of the microscope confocal head. Microscopes for using this type of contrast are then often equipped with a port called a “non-descanned port” which allows us to avoid all the losses generated by the numerous optical elements of the confocal head. Implementation may be eventually simpler than in classical confocal microscopy, yet it is still necessary to have a pulsed laser system capable of delivering sub-picosecond pulses in the near infrared.

Laser systems based upon solid-state gain media of the titanium doped sapphire type are now the most popular. There exist today laser systems particularly optimized for nonlinear microscopy, notably with a range of tunability stretching from less than 700 to over 1,000 nm. More and more, these systems also offer the possibility of pre-compensating the dispersion of laser pulses in the optical components crossed in microscopes and therefore guarantee a pulse duration which is as short as possible. Finally, many fluorescent probes used classically with linear methods are also capable of two-photon absorption, but the absorption mechanism is quite different. It is not guaranteed that a good fluorophore used in confocal microscopy is also a very good fluorophore for nonlinear absorption *(*and vice versa). The effective implementation of this technique therefore requires a good knowledge of nonlinear properties of molecular probes; the bibliography on the subject today is particularly well supplied.

If this mode of microscopy does not seem very complicated to implement technically, it requires very expensive equipment whose price must be justified by the increased opportunities and major scientific output over conventional confocal microscopy. It is therefore necessary to understand the fundamental contributions of these modes of contrast which are not always obvious to the neophyte.

Firstly, it is obviously not the simple "self-confocality" that makes nonlinear contrasts so interesting. Using laser systems ten times more expensive to do without a simple pinhole is not a very convincing argument! The advantages of nonlinear modes of contrast lie firstly in the use of an excitation in the near infrared instead of the usual visible. In this range of wavelengths, biological tissues absorb very little and scatter less. The excitation beam is less altered by the superficial tissue layers before getting to the plane of focus. In addition, the spectral separation between excitation and collection is much simpler and more effective because, firstly, the backscatter of the excitation beam is reduced and, secondly, the excitation light is in the near-infrared spectral region, a long way from the excited absorption bands.

Another major advantage of this type of contrast is that the infrared beam interacts less with the tissues and induces possible photochemical damage only at the focal plane, where the mechanism of nonlinear absorption is dominant. Indeed, the focal plane is still subject to damage by photochemical mechanisms, but when performing stacks of images, for example, each plane

will only be excited once. As a result, these specificities help to give nonlinear microscopy two major advantages: a greater depth of penetration and a reduced invasivity. The first point is explained by the fact that the signal-to-noise ratio is greatly improved by the localized emission because it is no longer necessary to remove the fluorescence outside the focal plane: it virtually no longer exists. In addition, the excitation beam is less disturbed when passing through the tissues up to the focal volume since the nonlinear absorption phenomenon takes place only in the focal volume and the absorption and tissue scattering are weaker in the infrared. Consequently, the signal-to-noise ratio is improved, but also, more robust to an increase in the imaging depth. Thanks to this greater capacity of penetration and less invasivity compared with classical confocal microscopy, the nonlinear contrasts are particularly suited to working on samples of living tissue or even directly on small living animals [NAS 05].

However, there remains a theoretical limit to the depth of penetration. It is known that the light scattering (and to a lesser extent absorption) theoretically causes an exponential decrease in the power of the excitation beam as a function of penetration depth. On the other hand, the focusing of the laser beam creates the opposite effect: a quadratic growth of the power density per unit of surface (which determines the probability of nonlinear absorption). It is therefore the scattering which prevails and there always comes a time when the power density at the focal volume becomes comparable with the power density on the sample surface. In this case, the fluorescence from the focal volume (signal) becomes comparable with the surface fluorescence (noise), which moves the contrast of images towards one.

The theoretical limit of penetration has been studied [THE 03], as well as parameters that can influence the imaging depth [OHE 01]. The essential element for maximizing the penetration depth is to have a long working distance objective (of the order of a millimeter) and especially of high numerical aperture (of the order of one) in order that the power density increases as quickly as possible to attempt to compensate as much as possible for the exponential loss due to scattering. For certain types of weakly scattering samples, such as the brain, a maximum imaging depth of the order of a millimeter has been demonstrated [THE 03]. However, in this particular case, the maximum imaging depth could have only been achieved by using a rather unusual laser system (regenerative amplifier) to deliver peak power pulses which are large enough.

Today, most multiphotonic microscopy systems are equipped with Ti: Al_2O_3 oscillators which do not have sufficient peak power to excite a nonlinear mechanism at such depths. Consequently, for a given labeling, the imaging depth in multiphotonic microscopy is theoretically limited by the properties of scattering and absorption of the samples, but in practice, it is rare that the available laser systems provide sufficient peak power to reach this theoretical limit. In conclusion, it is now clear that nonlinear microscopy can achieve imaging depths greater than classical confocal microscopy [CEN 98].

In classical confocal microscopy, it is difficult to reach imaging depths exceeding 50 microns [DAI 06], although some studies presents quite noisy images at depths of the order of 100 microns [COL 05]. In contrast, in multiphotonic microscopy, it is not uncommon to exceed a hundred microns or reach imaging depths of the order of 600-800 microns in weakly scattering samples such as the brain [HEL 05]. In terms of resolution and not penetration, it should be emphasized that a misunderstanding may remain between optical physicists and biologists, the latter sometimes thinking that this new type of contrast will enable them to achieve a better resolution. However, it is quite the opposite which happens: the use of an excitation in the near infrared has the effect of creating a focal volume which is more important than with the classical confocal contrast since the diameter of the Airy pattern is proportional to the wavelength. However, because of the nonlinearity of the absorption phenomenon, there is a slight contraction of the distribution of fluorescence compared with the illumination function and the overall lateral resolution remains similar (although slightly higher) to the lateral resolution in classical confocal microscopy [ZIP 03]. The axial resolution, meanwhile, is not coming from spatial filtering but from the nonlinear effect coupled to strong focusing of the beam. The axial resolution is therefore not determined as in the case of classical confocal microscopy. However, we find similar values [ZIP 03]. Again, the essential contribution of the nonlinear contrast is less invasivity and greater penetration capability owing to the greater robustness of the signal-to-noise ratio in relation to the penetration depth.

Other nonlinear properties have been used in scanning microscopy, such as second harmonic generation [FRA 61]. In this nonlinear mechanism, two photons at a wavelength λ interact in a material to generate a new photon with double the energy (therefore wavelength $\lambda/2$). This mechanism of interaction differs drastically from two-photon absorption to the extent that it

is not an absorption followed by a mechanism of spontaneous emission. Second harmonic generation is a coherent frequency conversion process in which the converted photons are in phase with the incident photons. The light emitted by frequency conversion can easily be discriminated from light emitted by fluorescence because it is emitted at exactly $\lambda/2$, a wavelength at which substantially no photon can be emitted by fluorescence after absorption of two photons at λ (Stokes shift). In addition, it should be noted that this process is coherent and that the generated light therefore retains a "memory" of the incident photons. Therefore, it is emitted mainly in the direction of the incident beam and can interfere with itself or with the incident beam. The physico-chemical properties necessary for this interaction are not the same as for two-photon absorption. In particular, it is necessary that the material in which the frequency conversion takes place is not centrosymmetric (no center of symmetry). So this phenomenon is observable in anisotropic crystals, in some molecular structures with particular symmetries, but also at the interface between two isotropic media (owing to a local breakdown of symmetry). This feature also makes the process of second harmonic generation very sensitive to the incident polarization. In biological tissues, it is mainly the collagen (which has a helical structure) which is responsible for the second harmonic generation [CAM 02, ROT 79]. This specificity makes this contrast very popular because it allows, without any prior labeling, a protein which is the most abundant in the human body to be imaged.

The contrast with second harmonic generation can also be used with membranes labeled with "push-pull" dyes. These amphiphilic dyes are inserted into the lipid membranes in a certain direction. Thus, second harmonic generation is possible in simple lipid membranes, but tends to cancel out by interference when it comes to bilipid membranes, which allows us to differentiate them [MOR 00]. There are other types of studies by second harmonic generation, but it is not always easy to find in living tissues other molecules which can generate a second harmonic signal. However, in plant biology, we can cite the case of cellulose or starch grains [COX 05].

It should be noted that the list of nonlinear effects used in microscopy does not stop there. For example, the more recent use of third harmonic generation contrast brings even newer features to observe in intact and unlabeled tissue. In particular, this contrast no longer requires the presence of a non-centrosymmetric medium, but cannot exist in a uniform and

isotropic medium, which makes it particularly interesting to probe heterogeneities [DEB 06, OLI 10]. The difficulty in implementing this type of contrast then lies essentially in the fact that it is necessary to excite the sample with a wavelength not two, but three times larger than the signal to be recovered. This requires the use of laser systems capable of emitting further into the infrared using, for example, optical parametric oscillators (OPO) coupled with traditional femtosecond systems. Finally, we cannot conclude this section without mentioning the Coherent Anti-Stokes Raman Scattering (CARS) microscopy [ADI 06]. This is about applying nonlinear microscopy to the principle of Raman spectroscopy which allows us to study the vibrational transitions of a molecule reflecting its chemical bonds. Raman scattering nevertheless remains a much weaker phenomenon than fluorescence. However, it is possible, through a complex nonlinear interaction, to enhance a scattering at a frequency $2\omega_s$-ω_p by exciting molecules with two coherent pulses at respective frequencies of ω_s and ω_p. However, this scattering will only occur if the difference ω_s-ω_p corresponds to vibrational transitions of the excited molecules. Consequently, by imposing a well chosen frequency difference ω_s-ω_p, corresponding to a vibrational transition specific for a particular chemical bond, only molecules with the chemical bond are capable of emitting light at a frequency $2\omega_s$-ω_p. This method, although quite complex, is very interesting because, without the need for labeling, it offers a very high specificity in the localization or the study of chemical modifications of molecules of interest. However, CARS microscopy is not simple to implement, because on the one hand it requires the setting up of laser sources capable of delivering two coherent and tunable pulses relative to each other, and, on the other hand, because it is not always easy to find vibrational transitions which are both specific and exploitable.

To conclude on these aspects, we note that nonlinear microscopy has greatly diversified since the arrival of two-photon absorption microscopy, which, itself, is still the subject of active research. If two-photon absorption microscopy brings better depth imaging and less significant invasivity, it still requires the use of fluorescent labels (except in some cases). The additional and major contribution of other types of nonlinear microscopy is to be even more suitable for working *in vivo* because they are based mainly on endogenous nonlinear properties.

1.4.3. *Recent major advances: overcoming the diffraction limit*

This chapter on confocal laser scanning microscopy could not finish without mentioning the recent breakthroughs that are currently being developed in order to overcome the theoretical diffraction limit. These different techniques are referred to as super-resolution microscopy or even directly as "nanoscopies". The resolution limit of Abbe has long been seen as the absolute limit of optical microscopy. However, it is indeed possible, using structured illumination, interference or taking advantage of some special properties of fluorophores to obtain resolutions below 100 nm and, in some cases, 20 nm.

One of the first approaches in this field was done simply by interfering two light beams propagating in opposite directions with two face-to-face objectives. This method is known as the 4π–microscopy (referring to the solid angle of collection, close to 4π steradians in this case). The phenomenon of interference enables us not only to reduce the lateral resolution by modulating the intensity of the focal spot (three interference fringes with one more luminous in the center), but also to reduce the axial resolution in the same way. Thus, 4π–microscopy allows for lateral and axial resolution of the order of 100 nm [HEL 03].

Another approach was developed in the 1990s and is often accompanied by the 4π–configuration; this is STED microscopy (for STimulated Emission Depletion) [HEL 94]. This type of microscopy is based, not on a reduction of the illuminated area, but on a reduction in the size of the fluorescent spot with an inhibition of the emission on the periphery of the fluorescent pattern. To do this, two pulsed laser beams are used. The first beam allows a conventional two-photon excitation of the fluorescence. The second beam, in turn, is red-shifted and therefore cannot excite the fluorescence. However, it is able to trigger a mechanism of stimulated emission on the molecules already excited by the first beam. Thus, the role of the second beam is to inhibit the fluorescence of excited molecules by depleting them by a stimulated emission mechanism.

This configuration would, of course, have no interest if the second beam completely covered the first one. The second beam therefore has a particular spatial shape, in the form of a donut to deplete only the fluorescence in the periphery of the beam. Consequently, the collected fluorescence comes from a light spot smaller than the overall diameter of the first beam. However, it

should be noted that the spatial frequencies contained in the ring beam are also limited by diffraction. The central pattern cannot reach diameters of less than 100 nanometers. However, this problem is solved by a saturation phenomenon in the periphery of the beam. This reduces the size of the central zone which can then reach a size less than one hundred nanometers. This method, combined most often with 4π microscopy (which provides an increased axial resolution) has achieved resolutions of the order of 20 nm for biological samples and even achieved the record resolution of 6 nm on non-biological samples [HUA 10].

Finally, there is a second type of scanning laser approach which allows us to overcome the diffraction limit. These are the PALM (PhotoActivatable Localization Microscopy) and STORM (Stochastic Optical Reconstruction Microscopy) methods which are based upon similar principles [HUA 10, PAT 10]. It is no longer a case of restricting the emission region by inhibiting the fluorescence of neighbouring molecules, but directly, of activating fluorescence molecule by molecule. This is made possible through the use of photoactivatable molecules. The principle is the following: a light at a well-chosen wavelength allows photo-activating fluorescence (by sending a molecule of a given conformation, non-fluorescent, to another one, fluorescent). By using a low enough light power, it is possible to only photo-activate a few molecules, so that they are, on average, separated by a distance greater than the resolution of the microscope. The fluorescence is then collected as in all other methods, but on a photon counting camera. Thus, the N photons emitted by a single molecule are randomly distributed on the camera with the accuracy about their position determined by the optical resolution of the instrument. By determining the barycenter (or centroid) of all these points, it is possible to localize more accurately the position of the molecule. This localization is determined with an uncertainty equal to the optical resolution, but divided by the square root of the number N of emitted photons. After deactivation of the molecule or after waiting for it to lose its fluorescence by photobleaching, we can repeat the process for the other neighboring molecules and so on until we reconstruct a super-resolved sub-image of the focal volume. Again, the combined use of the 4π configuration achieves axial resolutions of the order of tens of nanometers and a lateral resolution of the same order [HUA 10].

Thus, thanks to these recent developments, optical microscopy achieves resolutions which begin to reach those of electron microscopy but also offers

the flexibility of fluorescent labeling, lower invasivity and the possibility of working on living biological material.

1.5. Bibliography

[BEC 06] BÉCHERRAWY T., *Optique Géométrique*, De Boeck University, Brussels, 2006.

[BOR 99] BORN M., WOLF E., *Principle of Optics*, Cambridge University Press, Cambridge, 1999.

[BOR 02] BORST J.W., VISSER A.J.W.G., "Fluorescence lifetime imaging microscopy in life science", *Measurement Science and Technology*, no. 21, p. 102002, 2010.

[CAM 02] CAMPAGNOLA P.J., MILLARD A.C., TERASAKI M., HOPPE P.E., MALONE C.J., MOHLER W.A., "Three-dimensional high-resolution second-harmonic generation imaging of endogenous structural proteins in biological tissues", *Biophysical Journal*, no. 81, p. 493-508, 2002.

[CEN 98] CENTONZE V.E., WHITE J.G., "Multiphoton excitation provides optical sections from deeper within scattering specimens than confocal imaging", *Biophysical Journal*, no. 75, p. 2015-2024, 1998.

[CHA 94] CHALFIE M., TU Y., EUSKIRCHEN G., WARD W.W., PRASHER D.C., "Green fluorescent protein as a marker for gene expression", *Science*, no. 263, p. 802-805, 1994.

[CHE 90] CHEONG W.F., PRAHL S.A., WELCH A.J., "A review of the optical properties of biological tissues", *IEEE Journal of Quantum Electronics*, no. 26, p. 2166-2185, 1990.

[COL 05] COLLIER T., FOLLEN M.M., A.,RICHARDS-KORTUM R., "Sources of scattering in cervical tissue: determination of the scattering coefficient by confocal microscopy", *Applied Optics*, no. 44, p. 2072-2081, 2005.

[CON 05] CONCHELLO J.A., "An overview of three-dimensional and four-dimensional microscopy by computational deconvolution", in STEPHENS D. (ed.), *Cell Imaging: Methods Express*, Scion, Oxford, 2005.

[COR 96] CORLE T.R., KINO G.S., *Confocal Scanning Optical Microscopy an Related Imaging Systems*, Academic Press, San Diego, CA, 1996.

[COX 05] COX G., MORENO N., FEIJO J., "Second-harmonic imaging of plant polysaccharides", *Journal of Biomedical Optics*, no. 10, 2005.

[DAI 06] DAILEY M.E., MANDERS E., SOLL D.R., TERASAKI M., "Confocal microscopy of living cells", in PAWLEY J.B. (ed.), *Handbook of Biological Confocal Microscopy*, 3rd edition, Springer Science+Business Media LLC, New York, 2006.

[DEB 06] DÉBARRE D., PENA A.M., SUPATTO W., BOULESTEIX T., STRUPLER M., SAUVIAT M.P., MARTIN J.L., SCHANNE-KLEIN M.C., BEAUREPAIRE E., "Microscopies multiharmoniques pour l'imagerie structurale de tissus intacts", *M/S: médecine sciences*, no. 22, p. 845-850, 2006.

[DEN 90] DENK W., STRICKLER J.H., WEBB W.W., "Two-photon laser scanning fluorescence microscopy", *Science*, no. 248, p. 73-76, 1990.

[DJA 06] DJAKER N., MARGUET D., RIGNEAULT H., "Microscopie Raman stimulée (CARS) : principes et applications", *M/S: médecine sciences*, no. 22, p. 853-858, 2006.

[DUN 96] DUNN A.K., SMITHPETER C., WELCH A.J., RICHARDS-KORTUM R., "Sources of contrast in confocal reflectance imaging", *Applied Optics*, no. 35, p. 3441-3446, 1996.

[FRA 61] FRANKEN P.A., HILL A.E., PETERS C.W., WEINREICH G., "Generation of Optical Harmonics", *Physical Review Letters*, no. 7, p. 118-119, 1961.

[GIB 91] GIBSON S.F., LANNI F., "Experimental test of an analytical model of aberration in an oil-immersion objective lens used in three-dimensional light microscopy", *Journal of the Optical Society of America A*, no. 8, p. 1601-1613, 1991.

[GOP 31] GÖPPERT-MAYER M., "Über Elementarakte mit zwei Quantensprüngen", *Annalen der Physik*, no. 401, p. 273-294, 1931.

[HAE 04] HAEBERLÉ O., "Focusing of light through a stratified medium: a practical approach for computing microscope point spread functions Part II: confocal and multiphoton microscopy", *Optics Communications*, no. 235, p. 1-10, 2004.

[HEC 02] HECHT E., *Optics*, Addison Wesley, San Francisco, CA, 2002.

[HEL 94] HELL S.W., WICHMANN J., "Breaking the diffraction resolution limit by stimulated emission: stimulated-emission-depletion fluorescence microscopy", *Optics Letters*, no. 19, p. 780-782, 1994.

[HEL 03] HELL S.W., "Toward fluorescence nanoscopy", *Nature Biotechnology* no. 21, p. 1347-1355, 2003.

[HEL 05] HELMCHEN F., DENK W., "Deep tissue two-photon microscopy", *Nature Methods*, no. 2, p. 932-940, 2005.

[HIB 04] HIBBS A.R., *Confocal Microscopy for Biologists*, Kluwer Academic/Plenum Publishers, New York, 2004.

[HOO 65] HOOKE R., *Micrographia: or, Some Physiological Descriptions of Minute Bodies Made by Magnifying Glasses*, J. Martyn and J. Allestry, London, 1665.

[HUA 10] HUANG B., BABCOCK H., ZHUANG X., "Breaking the diffraction barrier: Super-resolution imaging of cells", *Cell*, no. 143, p. 1047-1058, 2010.

[KOZ 01] KOZUBEK M., "Theoretical versus experimental resolution in optical microscopy", *Microscopy Research and Technique*, no. 53, p. 157-166, 2001.

[MAY 07] MAYEVSKY A., ROGATSKY G.G., "Mitochondrial function in vivo evaluated by NADH fluorescence: from animal models to human studies", *American Journal of Physiology – Cell Physiology*, no. 292, p. 615-640, 2007.

[MIN 57] MINSKY M., Microscopy apparatus, U.S. Patent 3013467, 1957.

[MOE 03] MOERNER W.E., FROMM D.P., "Methods of single-molecule fluorescence spectroscopy and microscopy", *Review of Scientific Instruments*, no. 74, p. 3597-3619, 2003.

[MOR 00] MOREAUX L., SANDRE O., BLANCHARD-DESCE M., MERTZ J., "Membrane imaging by simultaneous second-harmonic generation and two-photon microscopy", *Optics Letters*, no. 25, p. 320-322, 2000.

[NAS 05] NASE G., HELM P.J., REPPEN T., OTTERSEN O.P., "A multiphoton laser scanning microscope setup for transcranial in vivo imaging on mice", *Review of Scientific Instruments*, no. 76, p. 123702, 2005.

[OHE 01] OHEIM M., BEAUREPAIRE E., CHAIGNEAU E., MERTZ J., CHARPAK S., "Two-photon microscopy in brain tissue: parameters influencing the imaging depth", *Journal of Neuroscience Methods*, no. 111, p. 29-37, 2001.

[OLI 10] OLIVIER N., APTEL F., PLAMANN K., SCHANNE-KLEIN M.C., BEAUREPAIRE E., "Harmonic microscopy of isotropic and anisotropic microstructure of the human cornea", *Optics Express*, no. 18, p. 5028-5040, 2010.

[PAD 08] PADDOCK S., "Over the rainbow: 25 years of confocal imaging", *BioTechniques*, no. 44, p. 643-648, 2008.

[PAT 89] PATTERSON M.S., CHANCE B., WILSON B.C., "Time resolved reflectance and transmittance for the noninvasive measurement of tissue optical properties", *Applied Optics*, no. 28, p. 2331-2336, 1989.

[PAT 10] PATTERSON G.H., DAVIDSON M., MANLEY S., LIPPINCOTT-SCHWARTZ J., "Superresolution imaging using single-molecule localization", *Annual Review of Physical Chemistry*, no. 61, p. 345-367, 2010.

[PRA 03] PRASAD P.N., *Introduction to Biophotonics*, John Wiley & Sons, Hoboken, NJ, 2003.

[ROT 79] ROTH S., FREUND I., "Second harmonic generation in collagen", *Journal of Chemical Physics*, no. 70, p. 1637, 1979.

[SMI 98] SMITHPETER C.L., DUNN A.K., WELCH A.J., RICHARDS-KORTUM R., "Penetration depth limits of in vivo confocal reflectance imaging", *Applied Optics*, no. 37, p. 2750-2754, 1998.

[STE 98] STELZER E.H.K., "Contrast, resolution, pixelation, dynamic range and signal-to-noise ratio: fundamental limits to resolution in fluorescence light microscopy", *Journal of Microscopy*, no. 189, p. 15-24, 1998.

[THE 03] THEER P., HASAN M., DENK W., "Two-photon imaging to a depth of 1000µm in living brains by use of Ti:Al2O3 regenerative amplifier", *Optics Letters*, no. 28, p. 1022-1024, 2003.

[TÖR 97] TÖRÖK P., VARGA P., "Electromagnetic diffraction of light focused through a stratified medium", *Applied Optics*, no. 36, p. 2305-2312, 1997.

[TRU 04] TRUGNAN G., FONTANGES P., DELAUTIER D., AIT-SLIMANE T., "FRAP, FLIP, FRET, BRET, FLIM, PRIM... De nouvelles techniques pour voir la vie en couleur !", *M/S : médecine sciences*, no. 20, p. 1027-1034, 2004.

[TSI 98] TSIEN R.Y., "The green fluorescent protein", *Annual Review of Biochemistry*, no. 67, p. 509-544, 1998.

[TUR 91] TURRO N.J., *Modern Molecular Photochemistry*, University Science Books, Sausalito, CA, 1991.

[WAS 94] WASTIAUX G., *La microscopie optique moderne*, Tec & Doc, Cachan, 1994.

[WHI 87] WHITE J.G., AMOS W.B., "Confocal microscopy comes of age", *Nature*, no. 328, p. 183-184, 1987.

[YOO 06] YOO H., SONG I., GWEON D.G., "Measurement and restoration of the point spread function of fluorescence confocal microscpy", *Journal of Microscopy*, no. 221, p. 172-176, 2006.

[ZIP 03] ZIPFEL W.R., WILLIAMS R.M., WEBB W.W., "Nonlinear magic: multiphoton microscopy in the biosciences", *Nature Biotechnology*, no. 21, p. 1369-1377, 2003.